

# Synthesis and Characterization of an Isomorphous Lanthanide-Thiophenemonocarboxylate Series (Ln = La-Lu, except Pm) Amenable to Color Tuning

*Rami J. Batrice, Alyssa K. Adcock, Paula M. Cantos, Jeffery A. Bertke, Karah E. Knope\**

Department of Chemistry, Box 571227, Georgetown University, Washington, D.C. 20057

## Supporting Information

Reaction Optimization.....	2
Synthesis of La-1 – Lu-1.....	2
Mechanochemical Preparation of Nd-2.....	4
Crystallographic Refinement Details.....	4
Solid State Crystal Structures.....	10
Powder X-Ray Diffraction Patterns of La-1 – Lu-1.....	20
Emission and Excitation Spectra of La-1 – Lu-1.....	28
Raman Fluorescence.....	32
Time-Resolved Fluorescence Lifetime Measurements.....	33
Thermal Stability Measurements.....	35

## Reaction Optimization.

Optimization studies were performed by altering the reaction temperature to determine the ideal temperature regime for the formation of the title products. When running the reactions at low temperature (5 °C) for one week, the majority of starting material was unreacted, however, a small quantity of product formed as single crystals. Determination of the unit cells in the lanthanum, cerium, and europium products revealed crystal parameters identical to those found for **La-2**, informing of similar isomorphous compounds being formed as the kinetic product. Similar reactions were then performed at elevated temperature to optimize the formation of the pyridinium-containing products (**La-1** – **Lu-1**); the reaction mixture was kept constant and heated to 70 °C for three days. The reaction mixtures were then filtered while hot through a cotton plug and left in open vials to evaporate. Each of the lanthanide compounds crystallized over the next three to ten days, and were subsequently characterized by single crystal X-ray diffraction studies. The solid-state structures showed the formation of the desired isomorphous lanthanide solvate compounds, and powder X-ray diffraction analysis supported bulk purity of the isolated product.

## Synthesis of **La-1** – **Lu-1**.

$[(\text{La}(\text{TMC})_3(\text{H}_2\text{O})_2) \cdot (\text{HPy} \cdot \text{TMC})]_n$  (**La-1**). The product was synthesized according to the general procedure using 107.6 mg HTMC (0.84 mmol) and 998  $\mu\text{L}$  of a 205 mM  $\text{La}(\text{NO}_3)_3 \cdot 6\text{H}_2\text{O}$  solution (0.20 mmol). Colorless single crystals formed after 7 days as rectangular blocks which were harvested in a 59% yield (90 mg). Elemental Analysis: Calcd for  $\text{C}_{25}\text{H}_{22}\text{NO}_{10}\text{S}_4\text{La}$ : C, 39.32; H, 2.90; N, 1.83. Found: C, 39.04; H, 2.86; N, 1.91.

$[(\text{Ce}(\text{TMC})_3(\text{H}_2\text{O})_2) \cdot (\text{HPy} \cdot \text{TMC})]_n$  (**Ce-1**). The product was synthesized according to the general procedure using 104.7 mg HTMC (0.82 mmol) and 979  $\mu\text{L}$  of a 203 mM  $\text{Ce}(\text{NO}_3)_3 \cdot 6\text{H}_2\text{O}$  solution (0.20 mmol). Colorless rectangular blocks deposited after 8 days which were harvested in a 56% yield (87 mg). Elemental Analysis: Calcd for  $\text{C}_{25}\text{H}_{22}\text{NO}_{10}\text{S}_4\text{Ce}$ : C, 39.32; H, 2.90; N, 1.83. Found: C, 39.18; H, 2.75; N, 1.74.

$[(\text{Pr}(\text{TMC})_3(\text{H}_2\text{O})_2) \cdot (\text{HPy} \cdot \text{TMC})]_n$  (**Pr-1**). The product was synthesized according to the general procedure using 106.1 mg HTMC (0.83 mmol) and 989  $\mu\text{L}$  of a 204 mM  $\text{Pr}(\text{NO}_3)_3 \cdot 6\text{H}_2\text{O}$  solution (0.20 mmol). Pale green block-shaped crystals formed after 5 days which were harvested in a 65% yield (100 mg). Elemental Analysis: Calcd for  $\text{C}_{25}\text{H}_{22}\text{NO}_{10}\text{S}_4\text{Pr}$ : C, 39.22; H, 2.90; N, 1.83. Found: C, 39.41; H, 3.35; N, 1.59.

$[(\text{Nd}(\text{TMC})_3(\text{H}_2\text{O})_2) \cdot (\text{HPy} \cdot \text{TMC})]_n$  (**Nd-1**). The product was synthesized according to the general procedure using 101.5 mg HTMC (0.79 mmol) and 928  $\mu\text{L}$  of a 208 mM  $\text{Nd}(\text{NO}_3)_3 \cdot 6\text{H}_2\text{O}$  solution (0.19 mmol). Pale blue single crystals deposited as rectangular blocks after 5 days and were harvested in a 61% yield (91 mg). Elemental Analysis: Calcd for  $\text{C}_{25}\text{H}_{22}\text{NO}_{10}\text{S}_4\text{Nd}$ : C, 39.05; H, 2.88; N, 1.82. Found: C, 38.89; H, 2.88; N, 1.88.

$[(\text{Sm}(\text{TMC})_3(\text{H}_2\text{O})_2) \cdot (\text{HPy} \cdot \text{TMC})]_n$  (**Sm-1**). The product was synthesized according to the general procedure using 119.6 mg HTMC (0.93 mmol) and 874  $\mu\text{L}$  of a 260 mM  $\text{Sm}(\text{NO}_3)_3 \cdot 6\text{H}_2\text{O}$  solution (0.23 mmol). Colorless rectangular block crystals formed after 4 days

which were harvested in a 72% yield (128 mg). Elemental Analysis: Calcd for  $C_{25}H_{22}NO_{10}S_4Sm$ : C, 38.74; H, 2.86; N, 1.81. Found: C, 38.54; H, 2.95; N, 1.90.

$[(Eu(TMC)_3(H_2O)_2)(HPy \cdot TMC)]_n$  (**Eu-1**). The product was synthesized according to the general procedure using 105.9 mg HTMC (0.83 mmol) and 996  $\mu$ L of a 202 mM  $Eu(NO_3)_3 \cdot 6H_2O$  solution (0.20 mmol). Single crystals formed after 3 days as colorless rectangular blocks which were harvested in a 84% yield (131 mg). Elemental Analysis: Calcd for  $C_{25}H_{22}NO_{10}S_4Eu$ : C, 38.66; H, 2.86; N, 1.80. Found: C, 38.59; H, 2.66; N, 1.87.

$[(Gd(TMC)_3(H_2O)_2)(HPy \cdot TMC)]_n$  (**Gd-1**). The product was synthesized according to the general procedure using 107.0 mg HTMC (0.83 mmol) and 989  $\mu$ L of a 206 mM  $Gd(NO_3)_3 \cdot 6H_2O$  solution (0.20 mmol). Colorless rectangular blocks formed after 3 days and were harvested in an 81% yield (129 mg). Elemental Analysis: Calcd for  $C_{25}H_{22}NO_{10}S_4Gd$ : C, 38.40; H, 2.84; N, 1.79; Found: C, 38.36; H, 2.96; N, 1.92.

$[(Tb(TMC)_3(H_2O)_2)(HPy \cdot TMC)]_n$  (**Tb-1**). The product was synthesized according to the general procedure using 108.0 mg HTMC (0.84 mmol) and 998  $\mu$ L of a 206 mM  $Tb(NO_3)_3 \cdot 6H_2O$  solution (0.21 mmol). Colorless rectangular block crystals formed after 3 days which were harvested in an 82% yield (132 mg). Elemental Analysis: Calcd for  $C_{25}H_{22}NO_{10}S_4Tb$ : C, 38.32; H, 2.83; N, 1.79. Found: C, 38.25; H, 2.92; N, 1.87.

$[(Dy(TMC)_3(H_2O)_2)(HPy \cdot TMC)]_n$  (**Dy-1**). The product was synthesized according to the general procedure using 106.4 mg HTMC (0.83 mmol) and 972  $\mu$ L of a 208 mM  $Dy(NO_3)_3 \cdot 6H_2O$  solution (0.20 mmol). Colorless rectangular block single crystals formed after 5 days which were harvested in a 78% yield (125 mg). Elemental Analysis: Calcd for  $C_{25}H_{22}NO_{10}S_4Dy$ : C, 38.15; H, 2.82; N, 1.78. Found: C, 38.05; H, 2.68; N, 1.80.

$[(Ho(TMC)_3(H_2O)_2)(HPy \cdot TMC)]_n$  (**Ho-1**). The product was synthesized according to the general procedure using 111.8 mg HTMC (0.87 mmol) and 991  $\mu$ L of a 215 mM  $Ho(NO_3)_3 \cdot 6H_2O$  solution (0.21 mmol). Pink rectangular block crystals formed after 6 days which were harvested in a 70% yield (118 mg). Elemental Analysis: Calcd for  $C_{25}H_{22}NO_{10}S_4Ho$ : C, 38.03; H, 2.81; N, 1.77. Found: C, 38.09; H, 2.87; N, 1.88.

$[(Er(TMC)_3(H_2O)_2)(HPy \cdot TMC)]_n$  (**Er-1**). The product was synthesized according to the general procedure using 102.5 mg HTMC (0.80 mmol) and 869  $\mu$ L of a 224 mM  $Er(NO_3)_3 \cdot 6H_2O$  solution (0.20 mmol). Pale pink single crystals formed as rectangular blocks after 5 days which were harvested in a 67% yield (103 mg). Elemental Analysis: Calcd for  $C_{25}H_{22}NO_{10}S_4Er$ : C, 37.92; H, 2.80; N, 1.77. Found: C, 38.06; H, 2.85; N, 1.90.

$[(Tm(TMC)_3(H_2O)_2)(HPy \cdot TMC)]_n$  (**Tm-1**). The product was synthesized according to the general procedure using 103.6 mg HTMC (0.81 mmol) and 979  $\mu$ L of a 201 mM  $Tm(NO_3)_3 \cdot 6H_2O$  solution (0.20 mmol). Colorless rectangular blocks formed after 4 days which were harvested in a 59% yield (93 mg). Elemental Analysis: Calcd for  $C_{25}H_{22}NO_{10}S_4Tm$ : C, 37.84; H, 2.79; N, 1.76. Found: C, 37.78; H, 2.87; N, 1.85.

$[(\text{Yb}(\text{TMC})_3(\text{H}_2\text{O})_2)\cdot(\text{HPy}\cdot\text{TMC})]_n$  (**Yb-1**). The product was synthesized according to the general procedure using 127.6 mg HTMC (1.00 mmol) and 820  $\mu\text{L}$  of a 296 mM  $\text{Yb}(\text{NO}_3)_3\cdot 6\text{H}_2\text{O}$  solution (0.24 mmol). Colorless rectangular blocks deposited after 8 days which were harvested in a 54% yield (105 mg). Elemental Analysis: Calcd for  $\text{C}_{25}\text{H}_{22}\text{NO}_{10}\text{S}_4\text{Yb}$ : C, 37.64; H, 2.78; N, 1.76. Found: C, 37.61; H, 2.85; N, 1.82.

$[(\text{Lu}(\text{TMC})_3(\text{H}_2\text{O})_2)\cdot(\text{HPy}\cdot\text{TMC})]_n$  (**Lu-1**). The product was synthesized according to the general procedure using 108.8 mg HTMC (0.85 mmol) and 946  $\mu\text{L}$  of a 219 mM  $\text{Lu}(\text{NO}_3)_3\cdot 6\text{H}_2\text{O}$  solution (0.21 mmol). Colorless rectangular blocks formed after 10 days which were harvested in a 54% yield (89 mg). Elemental Analysis: Calcd for  $\text{C}_{25}\text{H}_{22}\text{NO}_{10}\text{S}_4\text{Lu}$ : C, 37.55; H, 2.77; N, 1.75. Found: C, 37.78; H, 2.84; N, 1.79.

### Mechanochemical Preparation of Nd-2.

In the course of improving the selectivity and yields of the **Ln-1** products, workup conditions were systematically studied, revealing the formation of unexpected byproducts as a consequence of the conditions used. When using the neodymium(III) compound (**Nd-1**) to investigate the byproduct formation, single crystals of **Nd-1** were first isolated. The crystals were ground in ethanol within a mortar and pestle then wicked away of solvent several times, and ultimately dried in air; while a significant amount of **Nd-1** remained present in the powder, the diffraction pattern showed gradual transformation to a compound isomorphous with **La-2** with successive washing/grinding, suggesting that this process results in the formation of  $[\text{Nd}(\text{TMC})_3(\text{HTMC})_2]_n$  (*vide infra*). To determine if this product could be formed by other methods, a similar batch of single crystals of **Nd-1** were again isolated. Thorough drying under vacuum and mechanical grinding using a mortar and pestle yielded a bluish-white powder which was analyzed using PXRD and identified as  $[\text{Nd}(\text{TMC})_3(\text{HTMC})_2]_n$ . Interestingly, drying or grinding alone proved insufficient to form this byproduct.

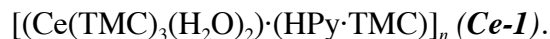
### Crystallographic Refinement Details.

Single crystals of each compound were mounted under paratone oil on a Mitegen micromount and immediately placed in a cold nitrogen stream prior to data collection. Data for compounds **Ce-1**, **Sm-1**, **Eu-1**, **Gd-1**, **Tb-1**, **Dy-1**, **Ho-1**, **Er-1**, and **Yb-1** were collected on a Bruker DUO equipped with an APEXII CCD detector and Mo fine-focus sealed source. Data for compounds **La-1**, **Pr-1**, **Nd-1**, **Tm-1**, **Lu-1**, and **La-2** were collected on a Bruker D8 Quest equipped with a Photon100 CMOS detector and a Mo ImS source. Data were collected using a combination of phi and omega scans and integrated with the Bruker SAINT program. Structure solutions were performed using the SHELXTL software suite. Intensities were corrected for Lorentz and polarization effects and an empirical absorption correction was applied using SADABS v2014/4 (TWINABS v2012/1 for **Lu-1**). Non-hydrogen atoms were refined with anisotropic thermal parameters and hydrogen atoms were included in idealized positions unless otherwise noted. Further comments on disorder models:

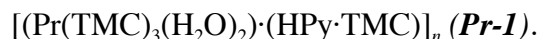
$[(\text{La}(\text{TMC})_3(\text{H}_2\text{O})_2)\cdot(\text{HPy}\cdot\text{TMC})]_n$  (**La-1**).

The thiophene ring portion of all three coordinated TMC ligands is disordered over two orientations. The like S-C and C-C bonds have been restrained to be similar. The free TMC anion is completely disordered over two orientations. The like S-C, C-C, and C-O distances

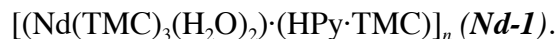
have been restrained to be similar. The two half occupancy pyridinium cations are each disordered about a symmetry site, thus they were refined with negative PART commands. Additionally, each cation is disordered over two positions. All of the pyridinium rings have been constrained to be ideal hexagons. Similar displacement amplitudes were imposed on disordered sites overlapping by less than the sum of van der Waals radii. Rigid-bond restraints were also imposed on displacement parameters for some disordered sites. The water H atoms were located in the difference map and the O-H distance was restrained to be 0.95Å. These H atoms refine to good hydrogen bonding positions. The pyridinium N-H hydrogen atoms could not be located in the difference map and thus were calculated in ideal positions.



The thiophene ring portion of all three coordinated TMC ligands is disordered over two orientations. The like S-C and C-C bonds have been restrained to be similar. The free TMC anion is completely disordered over two orientations. The like S-C, C-C, and C-O distances have been restrained to be similar. The two half occupancy pyridinium cations are each disordered about a symmetry site, thus they were refined with negative PART commands. Additionally, each cation is disordered over two positions. All of the pyridinium rings have been constrained to be ideal hexagons. Similar displacement amplitudes were imposed on disordered sites overlapping by less than the sum of van der Waals radii. Rigid-bond restraints were also imposed on displacement parameters for some disordered sites. The water H atoms were located in the difference map and the O-H distance was restrained to be 0.95Å. These H atoms refine to good hydrogen bonding positions. The pyridinium N-H hydrogen atoms could not be located in the difference map and thus were calculated in ideal positions.



The thiophene ring portion of all three coordinated TMC ligands is disordered over two orientations. The like S-C and C-C bonds have been restrained to be similar. The free TMC anion is completely disordered over two orientations. The like S-C, C-C, and C-O distances have been restrained to be similar. The two half occupancy pyridinium cations are each disordered about a symmetry site, thus they were refined with negative PART commands. Additionally, each cation is disordered over two positions. The disordered rings of pyridinium one have been constrained to be ideal hexagons. Similar displacement amplitudes were imposed on disordered sites overlapping by less than the sum of van der Waals radii. Rigid-bond restraints were also imposed on displacement parameters for some disordered sites. The water H atoms were located in the difference map and the O-H distance was restrained to be 0.95Å. These H atoms refine to good hydrogen bonding positions. The pyridinium N-H hydrogen atoms could not be located in the difference map and thus were calculated in ideal positions.



The thiophene ring portion of all three coordinated TMC ligands is disordered over two orientations. The like S-C and C-C bonds have been restrained to be similar. The free TMC anion is completely disordered over two orientations. The like S-C, C-C, and C-O distances have been restrained to be similar. The two half occupancy pyridinium cations are each disordered about a symmetry site, thus they were refined with negative PART commands. Additionally, pyridinium one is disordered over two positions and the rings have been constrained to be ideal hexagons. Similar displacement amplitudes were imposed on disordered

sites overlapping by less than the sum of van der Waals radii. Rigid-bond restraints were also imposed on displacement parameters for some disordered sites. The water H atoms were located in the difference map and the O-H distance was restrained to be 0.95Å. These H atoms refine to good hydrogen bonding positions. The pyridinium N-H hydrogen atoms could not be located in the difference map and thus were calculated in ideal positions.

$[(\text{Sm}(\text{TMC})_3(\text{H}_2\text{O})_2)\cdot(\text{HPy}\cdot\text{TMC})]_n$  (*Sm-1*).

The thiophene ring portion of all three coordinated TMC ligands is disordered over two orientations. The like S-C and C-C bonds have been restrained to be similar. The free TMC anion is completely disordered over two orientations. The like S-C, C-C, and C-O distances have been restrained to be similar. The two half occupancy pyridinium cations are each disordered about a symmetry site, thus they were refined with negative PART commands. Additionally, each cation is disordered over two positions. All of the pyridinium rings have been constrained to be ideal hexagons. The N1/C21B overlapping atom pair in cation one has been constrained to have equal x,y,z positions as well as equal anisotropic displacement parameters. Similar displacement amplitudes were imposed on disordered sites overlapping by less than the sum of van der Waals radii. Rigid-bond restraints were also imposed on displacement parameters for some disordered sites. The water H atoms were located in the difference map and the O-H distance was restrained to be 0.95Å. These H atoms refine to good hydrogen bonding positions. The pyridinium N-H hydrogen atoms could not be located in the difference map and thus were calculated in ideal positions.

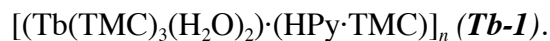
$[(\text{Eu}(\text{TMC})_3(\text{H}_2\text{O})_2)\cdot(\text{HPy}\cdot\text{TMC})]_n$  (*Eu-1*).

The thiophene ring portion of all three coordinated TMC ligands is disordered over two orientations. The like S-C and C-C bonds have been restrained to be similar. The free TMC anion is completely disordered over two orientations. The like S-C, C-C, and C-O distances have been restrained to be similar. The two half occupancy pyridinium cations are each disordered about a symmetry site, thus they were refined with negative PART commands. Additionally, pyridinium two is disordered over two positions and the rings have been constrained to be ideal hexagons. Similar displacement amplitudes were imposed on disordered sites overlapping by less than the sum of van der Waals radii. Rigid-bond restraints were also imposed on displacement parameters for some disordered sites. The water H atoms were located in the difference map and the O-H distance was restrained to be 0.95Å. These H atoms refine to good hydrogen bonding positions. The pyridinium N-H hydrogen atoms could not be located in the difference map and thus were calculated in ideal positions.

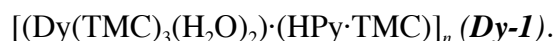
$[(\text{Gd}(\text{TMC})_3(\text{H}_2\text{O})_2)\cdot(\text{HPy}\cdot\text{TMC})]_n$  (*Gd-1*).

The thiophene ring portion of all three coordinated TMC ligands is disordered over two orientations. The like S-C and C-C bonds have been restrained to be similar. The free TMC anion is completely disordered over two orientations. The like S-C, C-C, and C-O distances have been restrained to be similar. The two half occupancy pyridinium cations are each disordered about a symmetry site, thus they were refined with negative PART commands. Additionally, pyridinium two is disordered over two positions and the rings have been constrained to be ideal hexagons. Similar displacement amplitudes were imposed on disordered sites overlapping by less than the sum of van der Waals radii. Rigid-bond restraints were also

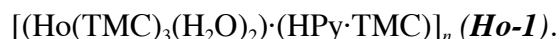
imposed on displacement parameters for some disordered sites. The water H atoms were located in the difference map and the O-H distance was restrained to be 0.95Å. These H atoms refine to good hydrogen bonding positions. The pyridinium N-H hydrogen atoms could not be located in the difference map and thus were calculated in ideal positions.



The thiophene ring portion of all three coordinated TMC ligands is disordered over two orientations. The like S-C and C-C bonds have been restrained to be similar. The free TMC anion is completely disordered over two orientations. The like S-C, C-C, and C-O distances have been restrained to be similar. The two half occupancy pyridinium cations are each disordered about a symmetry site, thus they were refined with negative PART commands. Additionally, each cation is disordered over two positions. The disordered rings of pyridinium two have been constrained to be ideal hexagons. Similar displacement amplitudes were imposed on disordered sites overlapping by less than the sum of van der Waals radii. Rigid-bond restraints were also imposed on displacement parameters for some disordered sites. The water H atoms were located in the difference map and the O-H distance was restrained to be 0.95Å. These H atoms refine to good hydrogen bonding positions. The pyridinium N-H hydrogen atoms could not be located in the difference map and thus were calculated in ideal positions.

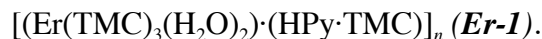


The thiophene ring portion of all three coordinated TMC ligands is disordered over two orientations. The like S-C and C-C bonds have been restrained to be similar. The free TMC anion is completely disordered over two orientations. The like S-C, C-C, and C-O distances have been restrained to be similar. The two half occupancy pyridinium cations are each disordered about a symmetry site, thus they were refined with negative PART commands. Additionally, each cation is disordered over two positions. The rings of pyridinium two have been constrained to be ideal hexagons. The N1/C21B overlapping atom pair in cation one has been constrained to have equal x,y,z positions as well as equal anisotropic displacement parameters. Similar displacement amplitudes were imposed on disordered sites overlapping by less than the sum of van der Waals radii. Rigid-bond restraints were also imposed on displacement parameters for some disordered sites. The water H atoms were located in the difference map and the O-H distance was restrained to be 0.95Å. These H atoms refine to good hydrogen bonding positions. The pyridinium N-H hydrogen atoms could not be located in the difference map and thus were calculated in ideal positions.

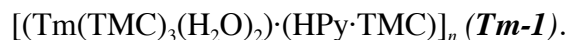


The thiophene ring portion of all three coordinated TMC ligands is disordered over two orientations. The like S-C and C-C bonds have been restrained to be similar. The free TMC anion is completely disordered over two orientations. The like S-C, C-C, and C-O distances have been restrained to be similar. The two half occupancy pyridinium cations are each disordered about a symmetry site, thus they were refined with negative PART commands. Additionally, each cation is disordered over two positions. All of the pyridinium rings have been constrained to be ideal hexagons. Similar displacement amplitudes were imposed on disordered sites overlapping by less than the sum of van der Waals radii. Rigid-bond restraints were also imposed on displacement parameters for some disordered sites. The water H atoms were located

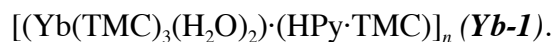
in the difference map and the O-H distance was restrained to be 0.95Å. These H atoms refine to good hydrogen bonding positions. The pyridinium N-H hydrogen atoms could not be located in the difference map and thus were calculated in ideal positions.



The thiophene ring portion of all three coordinated TMC ligands is disordered over two orientations. The like S-C and C-C bonds have been restrained to be similar. The free TMC anion is completely disordered over two orientations. The like S-C, C-C, and C-O distances have been restrained to be similar. The two half occupancy pyridinium cations are each disordered about a symmetry site, thus they were refined with negative PART commands. Additionally, pyridinium two is disordered over two positions and the rings have been constrained to be ideal hexagons. Similar displacement amplitudes were imposed on disordered sites overlapping by less than the sum of van der Waals radii. Rigid-bond restraints were also imposed on displacement parameters for some disordered sites. The water H atoms were located in the difference map and the O-H distance was restrained to be 0.95Å. These H atoms refine to good hydrogen bonding positions. The pyridinium N-H hydrogen atoms could not be located in the difference map and thus were calculated in ideal positions.



The thiophene ring portion of all three coordinated TMC ligands is disordered over two orientations. The like S-C and C-C bonds have been restrained to be similar. The free TMC anion is completely disordered over two orientations. The like S-C, C-C, and C-O distances have been restrained to be similar. The two half occupancy pyridinium cations are each disordered about a symmetry site, thus they were refined with negative PART commands. Additionally, pyridinium two is disordered over two positions and the rings have been constrained to be ideal hexagons. Similar displacement amplitudes were imposed on disordered sites overlapping by less than the sum of van der Waals radii. Rigid-bond restraints were also imposed on displacement parameters for some disordered sites. The water H atoms were located in the difference map and the O-H distance was restrained to be 0.95Å. These H atoms refine to good hydrogen bonding positions. The pyridinium N-H hydrogen atoms could not be located in the difference map and thus were calculated in ideal positions.



The thiophene ring portion of all three coordinated TMC ligands is disordered over two orientations. The like S-C and C-C bonds have been restrained to be similar. The free TMC anion is completely disordered over two orientations. The like S-C, C-C, and C-O distances have been restrained to be similar. The C17/C17B atom pair in the free TMC has been constrained to have equal x,y,z positions as well as equal anisotropic displacement parameters. The two half occupancy pyridinium cations are each disordered about a symmetry site, thus they were refined with negative PART commands. Additionally, cation two is disordered over two positions and the rings have been constrained to be ideal hexagons. Similar displacement amplitudes were imposed on disordered sites overlapping by less than the sum of van der Waals radii. The water H atoms were located in the difference map and the O-H distance was restrained to be 0.95Å. These H atoms refine to good hydrogen bonding positions. The

pyridinium N-H hydrogen atoms could not be located in the difference map and thus were calculated in ideal positions.

$[(\text{Lu}(\text{TMC})_3(\text{H}_2\text{O})_2) \cdot (\text{HPy} \cdot \text{TMC})]_n$  (**Lu-1**).

All crystals examined exhibited non-merohedral twinning. For the datum crystal two distinct domains were identified and refined to a ratio of approximately 60:40. The thiophene ring portion of all three coordinated TMC ligands is disordered over two orientations. The like S-C and C-C bonds have been restrained to be similar. The free TMC anion is completely disordered over two orientations. The like S-C, C-C, and C-O distances have been restrained to be similar. The two half occupancy pyridinium cations are each disordered about a symmetry site, thus they were refined with negative PART commands. Additionally, pyridinium two is disordered over two positions and the rings have been constrained to be ideal hexagons. Similar displacement amplitudes were imposed on disordered sites overlapping by less than the sum of van der Waals radii. Rigid-bond restraints were also imposed on displacement parameters for some disordered sites. The water H atoms were located in the difference map and the O-H distance was restrained to be 0.95 Å. These H atoms refine to good hydrogen bonding positions. The pyridinium N-H hydrogen atoms could not be located in the difference map and thus were calculated in ideal positions.

$[\text{La}(\text{TMC})_3(\text{HTMC})_2]_n$  (**La-2**).

The thiophene ring portion of all five TMC/HTMC ligands is disordered over two orientations. The like S-C and C-C bonds have been restrained to be similar. The C7/C7B, C12/C12B, and C17/C17B atom pairs, respectively, were constrained to have equal x,y,z positions as well as equal anisotropic displacement parameters. Similar displacement amplitudes were imposed on disordered sites overlapping by less than the sum of van der Waals radii. Rigid-bond restraints were also imposed on displacement parameters for some disordered sites. The hydroxyl H atoms were located in the difference map and the O-H distance was restrained to be 0.88 Å. These H atoms refine to good hydrogen bonding positions. The Flack ( $x = -0.013(5)$ ) and Hooft ( $y = -0.020(6)$ ) parameters are ambiguous, likely due to the large number of disordered sites in the model.

## Solid State Crystal Structures.

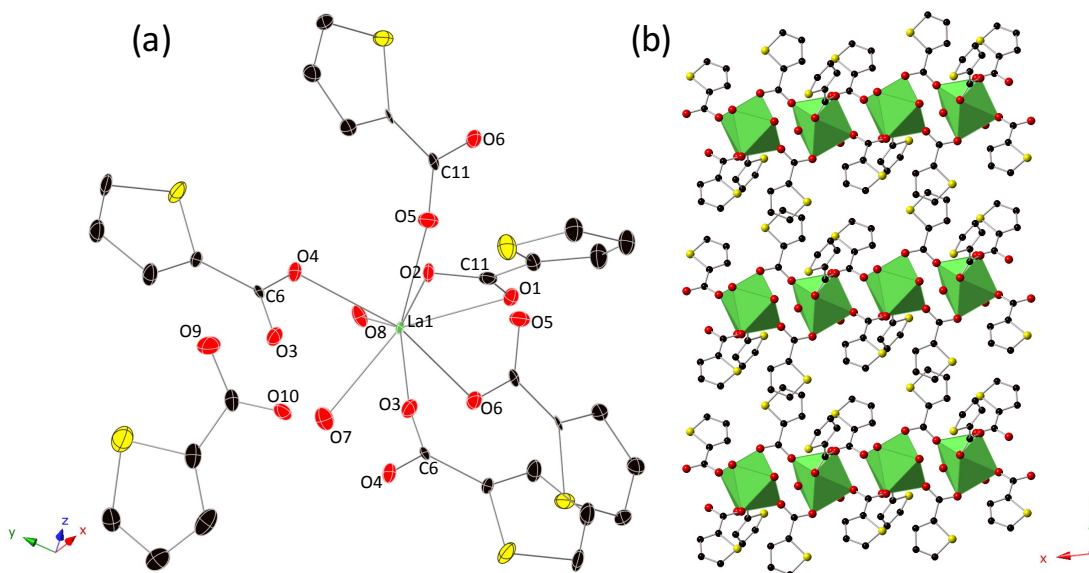


**Figure S1.** Crystal structure of  $[(\text{La}(\text{TMC})_3(\text{H}_2\text{O})_2) \cdot (\text{HPy} \cdot \text{TMC})]_n$  (**La-1**) shown as (a) thermal ellipsoid model of monomer unit and (b) packing diagram viewed along [001] direction. Hydrogen atoms and pyridinium ion are omitted for clarity, as well as outer sphere TMC in (b). Color code: La, green; C, black; O, red; S, bright yellow.

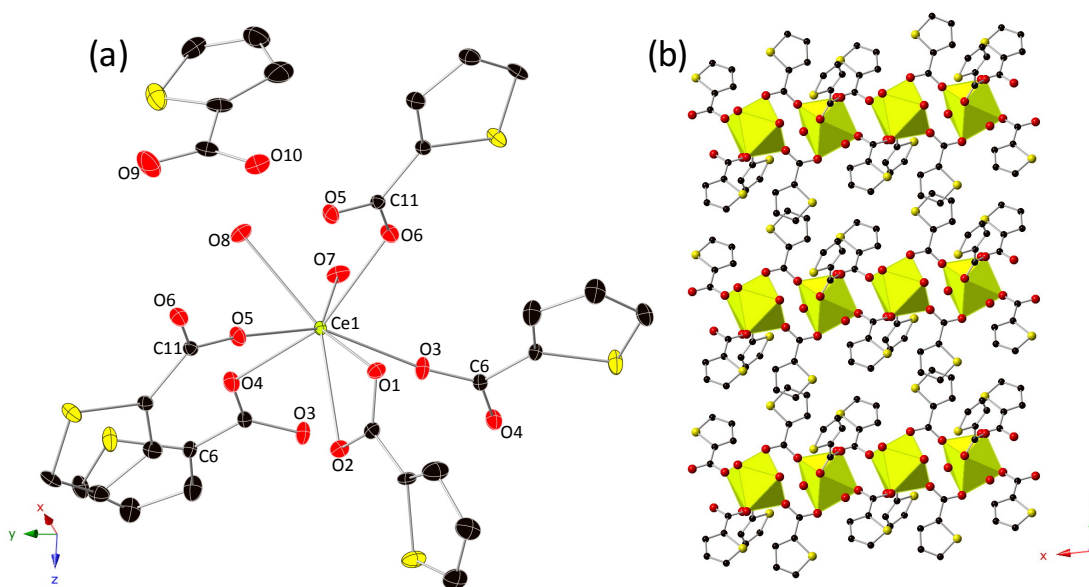


**Figure S2.** Crystal structure of  $[(\text{Ce}(\text{TMC})_3(\text{H}_2\text{O})_2) \cdot (\text{HPy} \cdot \text{TMC})]_n$  (**Ce-1**) shown as (a) thermal ellipsoid model of monomer unit and (b) packing diagram viewed along [001] direction. Hydrogen atoms and pyridinium ion are omitted for clarity, as well as outer sphere TMC in (b). Color code: Ce, lime green; C, black; O, red; S, bright yellow.

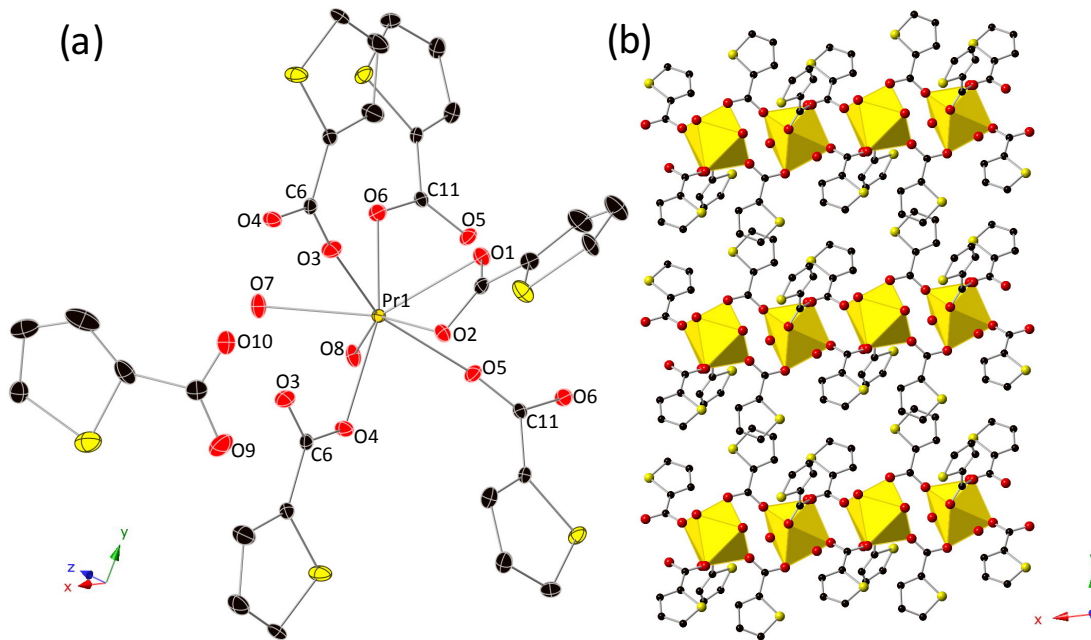


**Figure S3.** Crystal structure of  $[(Pr(TMC)_3(H_2O)_2) \cdot (HPy \cdot TMC)]_n$  (**Pr-1**) shown as (a) thermal ellipsoid model of monomer unit and (b) packing diagram viewed along [001] direction. Hydrogen atoms and pyridinium ion are omitted for clarity, as well as outer sphere TMC in (b). Color code: Pr, dark yellow; C, black; O, red; S, bright yellow.

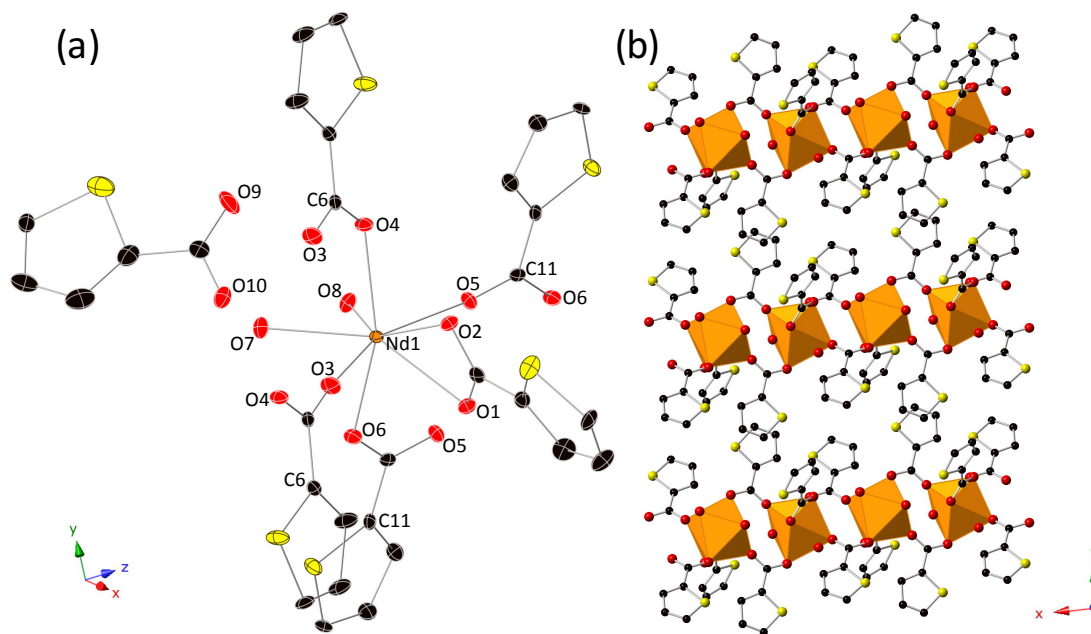


**Figure S4.** Crystal structure of  $[(Nd(TMC)_3(H_2O)_2) \cdot (HPy \cdot TMC)]_n$  (**Nd-1**) shown as (a) thermal ellipsoid model of monomer unit and (b) packing diagram viewed along [001] direction. Hydrogen atoms and pyridinium ion are omitted for clarity, as well as outer sphere TMC in (b). Color code: Nd, orange; C, black; O, red; S, bright yellow.

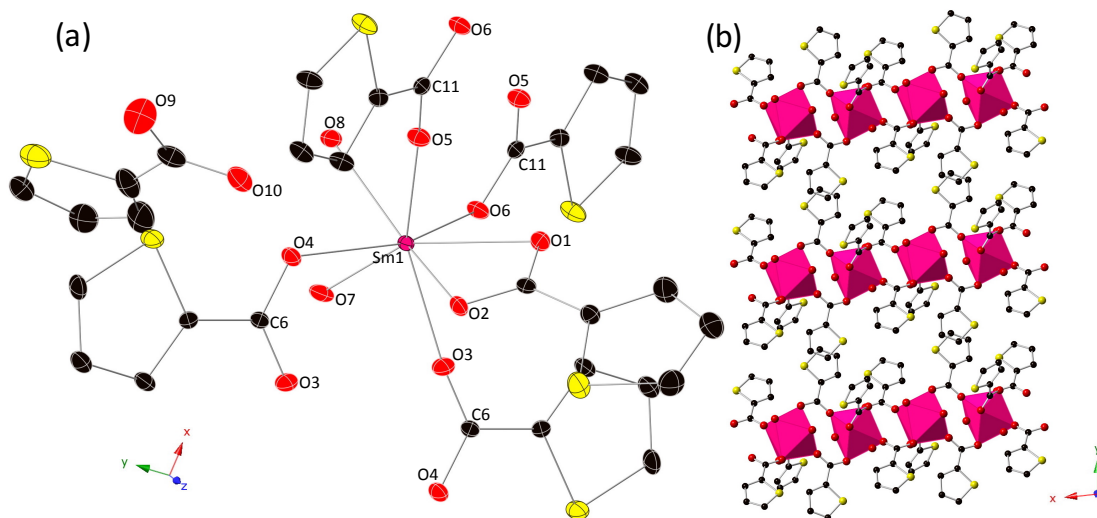


**Figure S5.** Crystal structure of  $[(\text{Sm}(\text{TMC})_3(\text{H}_2\text{O})_2) \cdot (\text{HPy} \cdot \text{TMC})]_n$  (**Sm-1**) shown as (a) thermal ellipsoid model of monomer unit and (b) packing diagram viewed along  $[001]$  direction. Hydrogen atoms and pyridinium ion are omitted for clarity, as well as outer sphere TMC in (b). Color code: Sm, magenta; C, black; O, red; S, bright yellow.

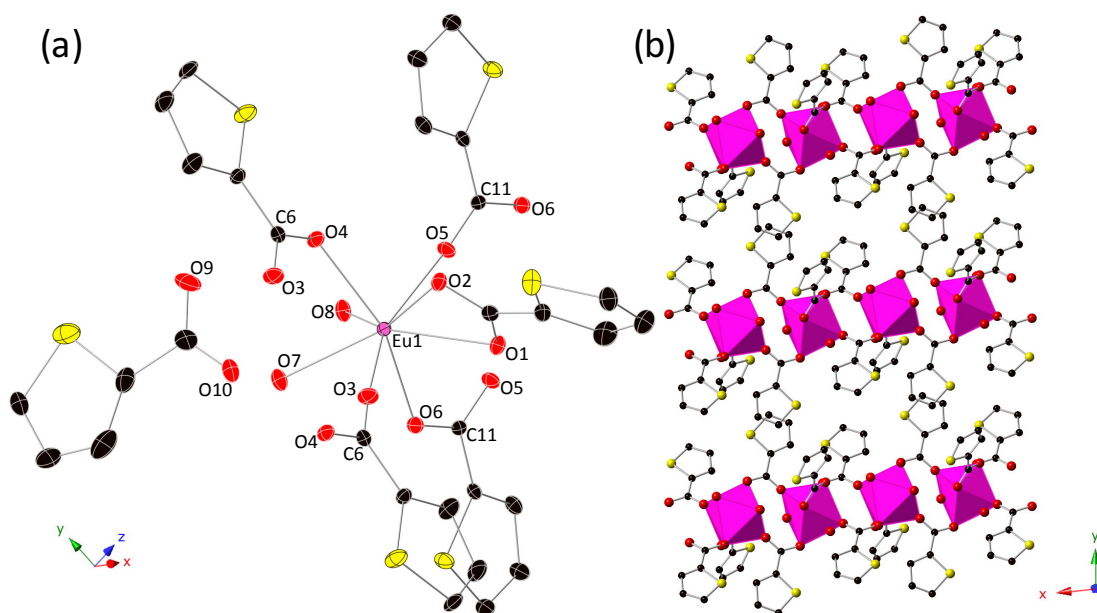


**Figure S6.** Crystal structure of  $[(\text{Eu}(\text{TMC})_3(\text{H}_2\text{O})_2) \cdot (\text{HPy} \cdot \text{TMC})]_n$  (**Eu-1**) shown as (a) thermal ellipsoid model of monomer unit and (b) packing diagram viewed along  $[001]$  direction. Hydrogen atoms and pyridinium ion are omitted for clarity, as well as outer sphere TMC in (b). Color code: Eu, pink; C, black; O, red; S, bright yellow.



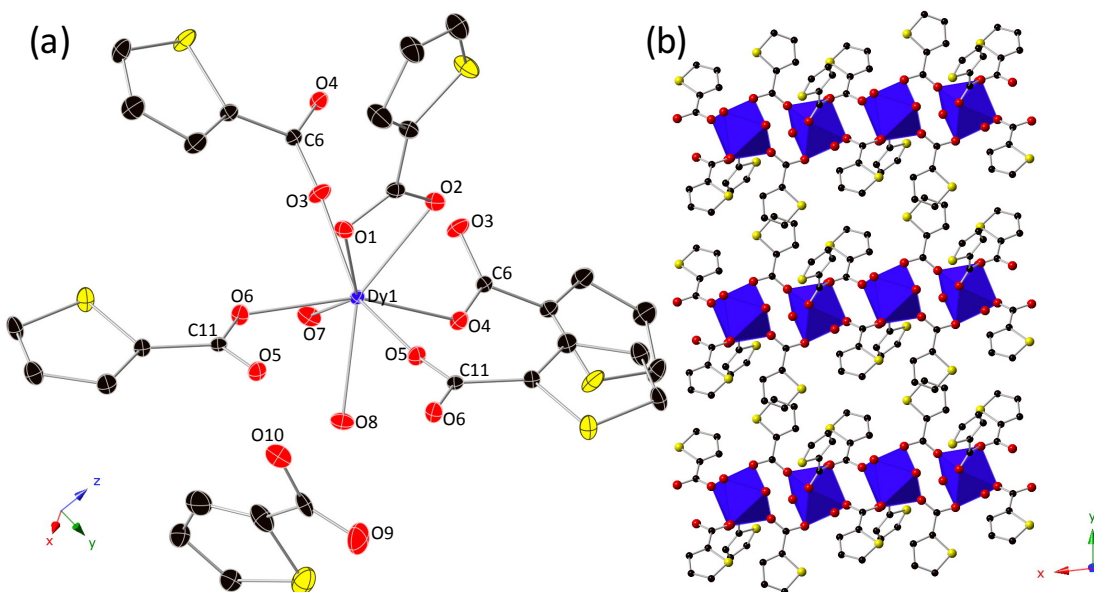


**Figure S9.** Crystal structure of  $[(\text{Dy}(\text{TMC})_3(\text{H}_2\text{O})_2) \cdot (\text{HPy} \cdot \text{TMC})]_n$  (**Dy-1**) shown as (a) thermal ellipsoid model of monomer unit and (b) packing diagram viewed along  $[001]$  direction. Hydrogen atoms and pyridinium ion are omitted for clarity, as well as outer sphere TMC in (b). Color code: Dy, blue; C, black; O, red; S, bright yellow.

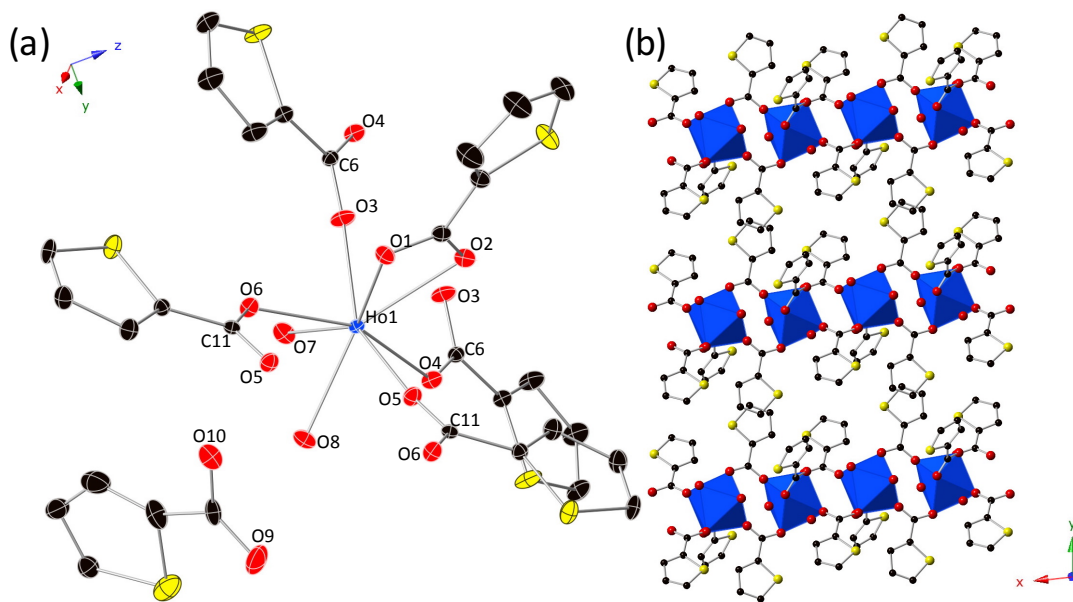


**Figure S10.** Crystal structure of  $[(\text{Ho}(\text{TMC})_3(\text{H}_2\text{O})_2) \cdot (\text{HPy} \cdot \text{TMC})]_n$  (**Ho-1**) shown as (a) thermal ellipsoid model of monomer unit and (b) packing diagram viewed along  $[001]$  direction. Hydrogen atoms and pyridinium ion are omitted for clarity, as well as outer sphere TMC in (b). Color code: Ho, blue; C, black; O, red; S, bright yellow.

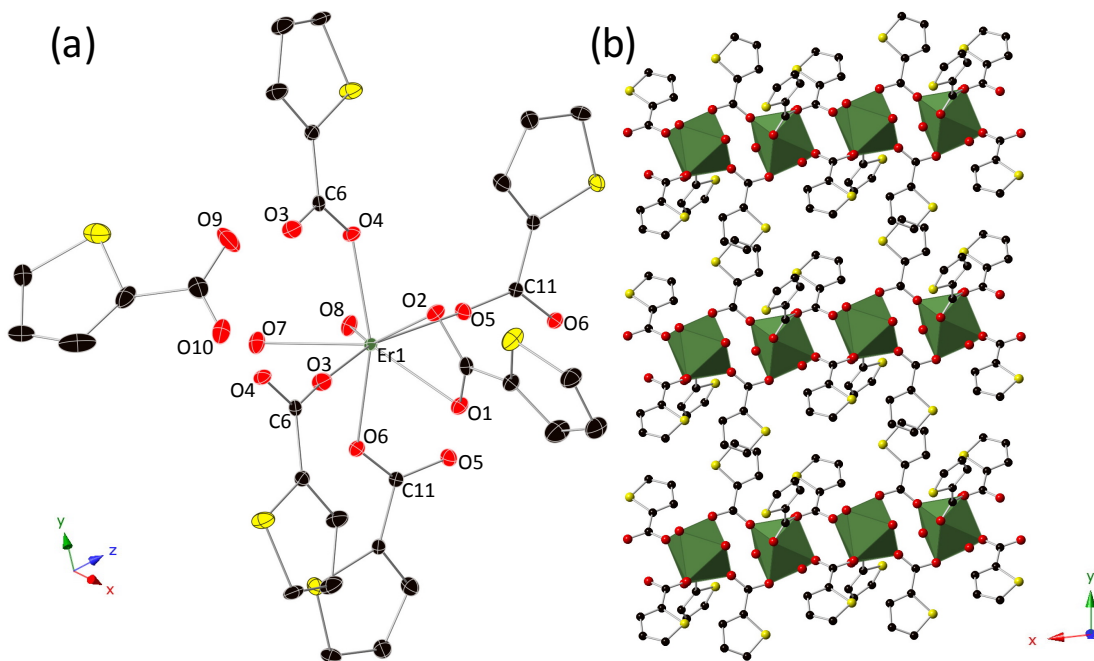


**Figure S11.** Crystal structure of  $[(\text{Er}(\text{TMC})_3(\text{H}_2\text{O})_2) \cdot (\text{HPy} \cdot \text{TMC})]_n$  (**Er-1**) shown as (a) thermal ellipsoid model of monomer unit and (b) packing diagram viewed along  $[001]$  direction. Hydrogen atoms and pyridinium ion are omitted for clarity, as well as outer sphere TMC in (b). Color code: Er, green; C, black; O, red; S, bright yellow.

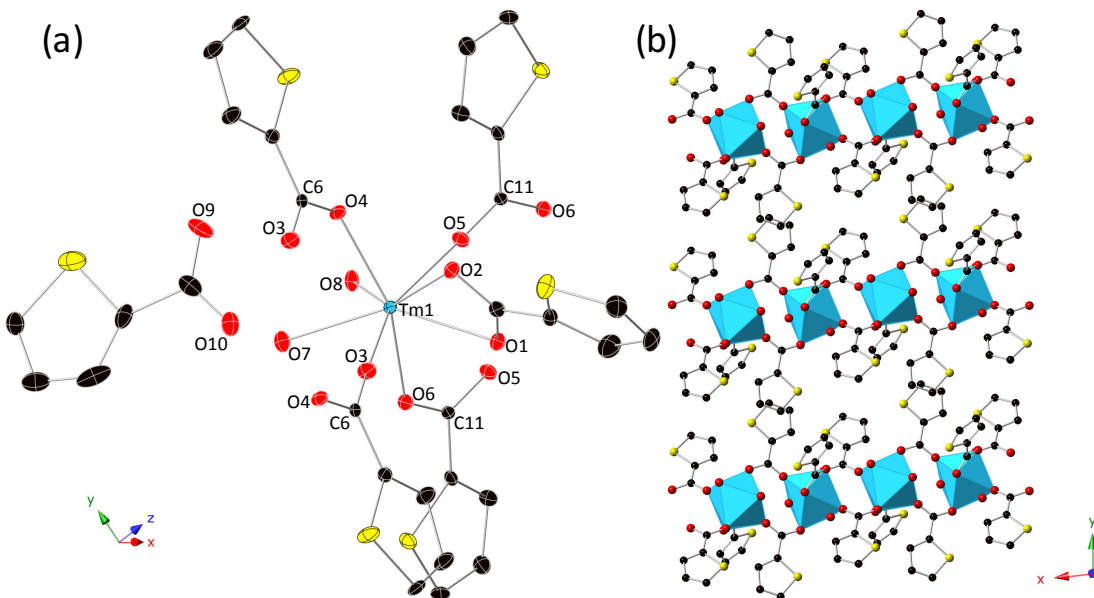


**Figure S12.** Crystal structure of  $[(\text{Tm}(\text{TMC})_3(\text{H}_2\text{O})_2) \cdot (\text{HPy} \cdot \text{TMC})]_n$  (**Tm-1**) shown as (a) thermal ellipsoid model of monomer unit and (b) packing diagram viewed along  $[001]$  direction. Hydrogen atoms and pyridinium ion are omitted for clarity, as well as outer sphere TMC in (b). Color code: Tm, light blue; C, black; O, red; S, bright yellow.

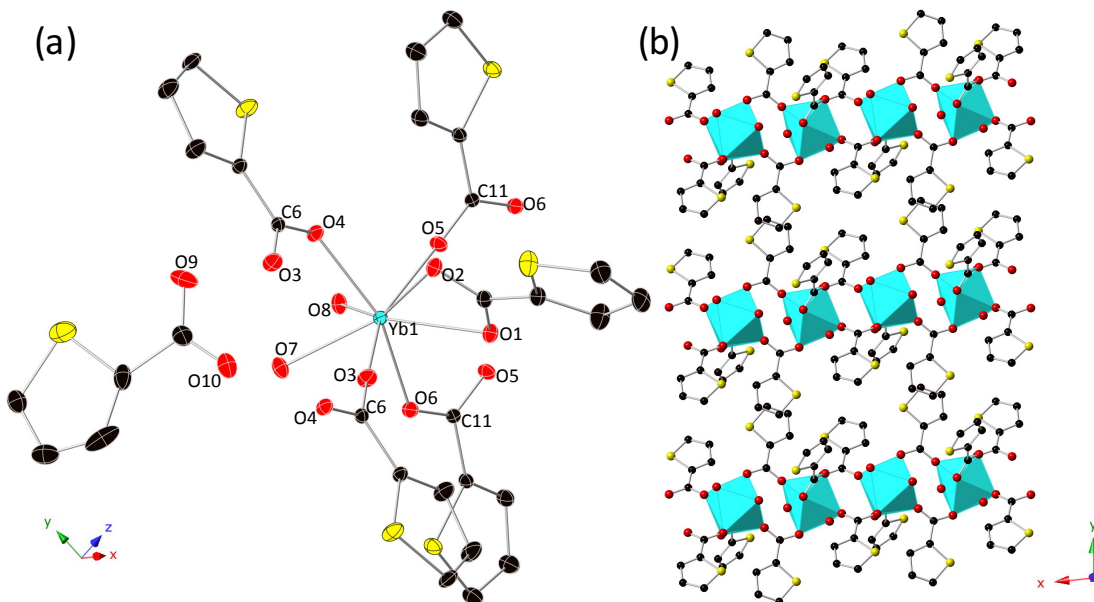


**Figure S13.** Crystal structure of  $[(\text{Yb}(\text{TMC})_3(\text{H}_2\text{O})_2) \cdot (\text{HPy} \cdot \text{TMC})]_n$  (**Yb-1**) shown as (a) thermal ellipsoid model of monomer unit and (b) packing diagram viewed along  $[001]$  direction. Hydrogen atoms and pyridinium ion are omitted for clarity, as well as outer sphere TMC in (b). Color code: Yb, light blue; C, black; O, red; S, bright yellow.

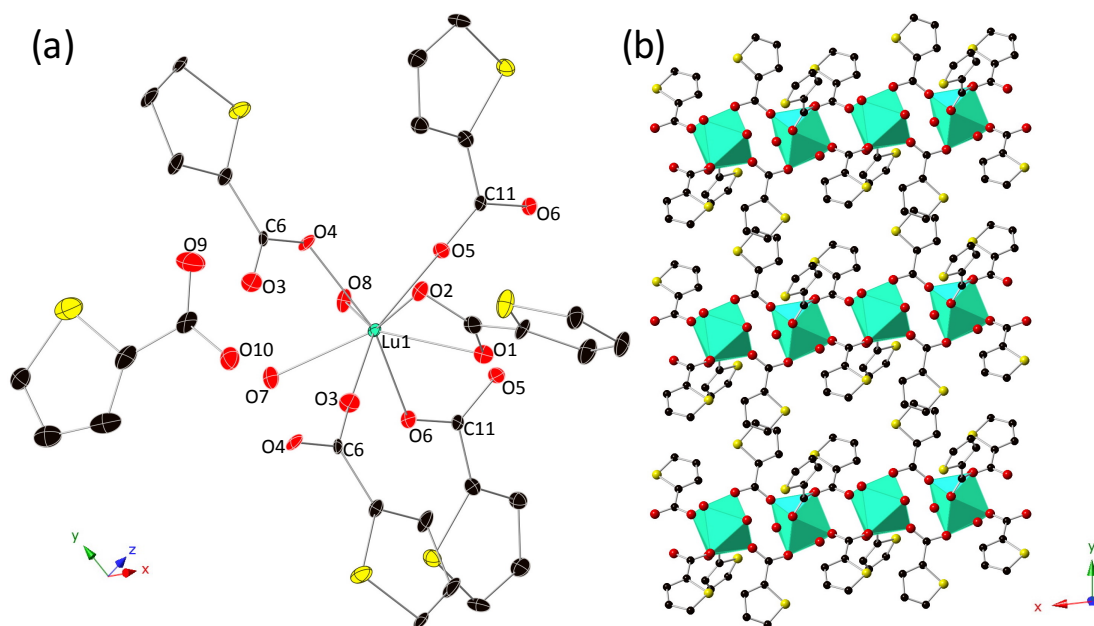


**Figure S14.** Crystal structure of  $[(\text{Lu}(\text{TMC})_3(\text{H}_2\text{O})_2) \cdot (\text{HPy} \cdot \text{TMC})]_n$  (**Lu-1**) shown as (a) thermal ellipsoid model of monomer unit and (b) packing diagram viewed along  $[001]$  direction. Hydrogen atoms and pyridinium ion are omitted for clarity, as well as outer sphere TMC in (b). Color code: Lu, teal; C, black; O, red; S, bright yellow.

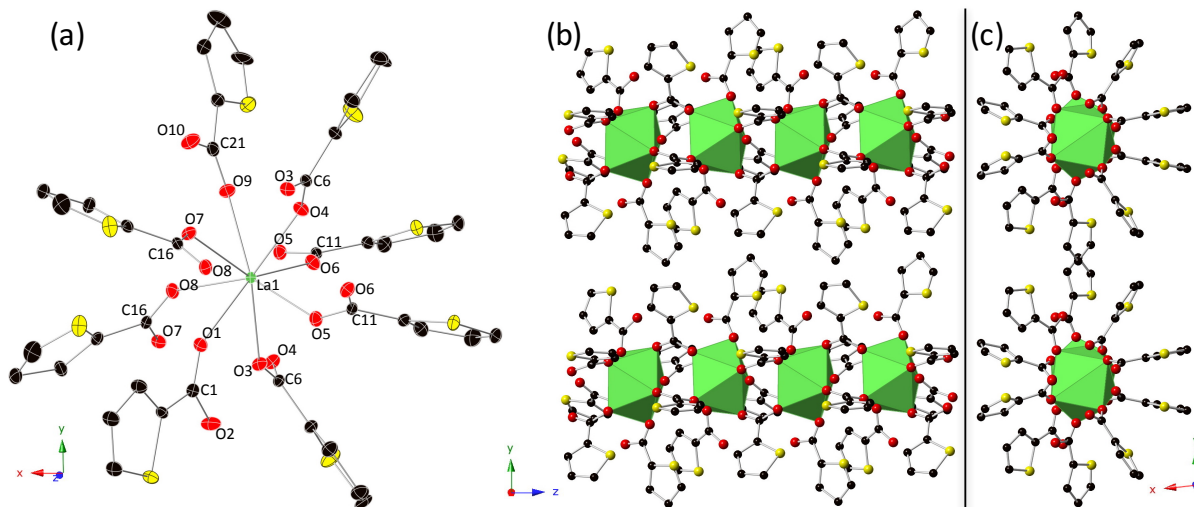


**Figure S15.** Crystal structure of  $[\text{La}(\text{TMC})_3(\text{HTMC})_2]_n$  (**La-2**) shown as (a) thermal ellipsoid model of monomer unit, (b) packing diagram viewed along  $[100]$  direction, and (c) packing diagram viewed along  $[001]$  direction. Hydrogen atoms and pyridinium ion are omitted for clarity, as well as outer sphere TMC in (b) and (c). Color code: La, teal; C, black; O, red; S, bright yellow.

**Table S1.** Selected bond lengths and angles of  $[(Ln(TMC)_3(H_2O)_2) \cdot (HPy \cdot TMC)]_n$  (**La-1 – Lu-1**) and  $[Ln(TMC)_3(HTMC)_2]_n$  (**La-2**).

Compound	bond	length (Å)	angle	$\theta$ (°)	Compound	bond	length (Å)	angle	$\theta$ (°)
<b>La-1</b>	La1-O1	2.594(4)	La1-O3-C6	167.9(4)	<b>Ce-1</b>	Ce1-O1	2.576(1)	Ce1-O3-C6	170.1(1)
	La1-O2	2.623(4)	La1i-O4-C6	118.0(4)		Ce1-O2	2.607(1)	Ce1i-O4-C6	120.52(9)
	La1-O3	2.428(4)	La1-O5-C11	169.0(4)		Ce1-O3	2.401(1)	Ce1-O5-C11	170.13(9)
	La1-O4i	2.505(4)	La1ii-O6-C11	120.2(4)		Ce1-O4i	2.472(1)	Ce1ii-O6-C11	121.12(9)
	La1-O5	2.440(3)				Ce1-O5	2.4156(9)		
	La1-O6ii	2.498(4)				Ce1-O6ii	2.477(1)		
	La1-O7	2.531(5)				Ce1-O7	2.509(1)		
	La1-O8	2.541(4)				Ce1-O8	2.525(1)		
	O7-H...O10	2.801(9)				O7-H...O10	2.797(2)		
O8-H...O10	2.693(8)			O8-H...O10	2.702(2)				
<b>Pr-1</b>	Pr1-O1	2.558(1)	Pr1-O3-C6	170.8(1)	<b>Nd-1</b>	Nd1-O1	2.539(2)	Nd1-O3-C6	171.1(2)
	Pr1-O2	2.589(1)	Pr1i-O4-C6	121.9(1)		Nd1-O2	2.570(2)	Nd1i-O4-C6	122.6(2)
	Pr1-O3	2.382(1)	Pr1-O5-C11	170.8(1)		Nd1-O3	2.365(2)	Nd1-O5-C11	171.1(2)
	Pr1-O4i	2.449(1)	Pr1ii-O6-C11	122.2(1)		Nd1-O4i	2.433(2)	Nd1ii-O6-C11	122.5(2)
	Pr1-O5	2.397(1)				Nd1-O5	2.378(2)		
	Pr1-O6ii	2.456(1)				Nd1-O6ii	2.442(2)		
	Pr1-O7	2.490(1)				Nd1-O7	2.476(2)		
	Pr1-O8	2.507(1)				Nd1-O8	2.482(2)		
	O7-H...O10	2.797(3)				O7-H...O10	2.787(5)		
O8-H...O10	2.704(2)			O8-H...O10	2.714(4)				
<b>Sm-1</b>	Sm1-O1	2.512(2)	Sm1-O3-C6	172.2(2)	<b>Eu-1</b>	Eu1-O1	2.501(2)	Eu1-O3-C6	172.8(2)
	Sm1-O2	2.545(2)	Sm1i-O4-C6	123.9(2)		Eu1-O2	2.537(2)	Eu1i-O4-C6	124.8(2)
	Sm1-O3	2.331(2)	Sm1-O5-C11	172.3(2)		Eu1-O3	2.312(2)	Eu1-O5-C11	172.2(2)
	Sm1-O4i	2.399(2)	Sm1ii-O6-C11	123.4(2)		Eu1-O4i	2.383(2)	Eu1ii-O6-C11	124.4(2)
	Sm1-O5	2.347(2)				Eu1-O5	2.329(2)		
	Sm1-O6ii	2.410(2)				Eu1-O6ii	2.397(2)		
	Sm1-O7	2.447(2)				Eu1-O7	2.433(2)		
	Sm1-O8	2.458(2)				Eu1-O8	2.451(2)		
	O7-H...O10	2.787(4)				O7-H...O10	2.787(4)		
O8-H...O10	2.719(3)			O8-H...O10	2.711(4)				
<b>Gd-1</b>	Gd1-O1	2.492(1)	Gd1-O3-C6	173.2(1)	<b>Tb-1</b>	Tb1-O1	2.479(1)	Tb1-O3-C6	173.9(1)
	Gd1-O2	2.525(1)	Gd1i-O4-C6	125.17(9)		Tb1-O2	2.518(1)	Tb1i-O4-C6	126.00(9)
	Gd1-O3	2.303(1)	Gd1-O5-C11	172.7(1)		Tb1-O3	2.285(1)	Tb1-O5-C11	172.9(1)
	Gd1-O4i	2.374(1)	Gd1ii-O6-C11	124.62(9)		Tb1-O4i	2.355(1)	Tb1ii-O6-C11	125.02(9)
	Gd1-O5	2.318(1)				Tb1-O5	2.302(1)		
	Gd1-O6ii	2.384(1)				Tb1-O6ii	2.367(1)		
	Gd1-O7	2.425(1)				Tb1-O7	2.412(1)		
	Gd1-O8	2.439(1)				Tb1-O8	2.423(1)		
	O7-H...O10	2.785(2)				O7-H...O10	2.785(2)		
O8-H...O10	2.720(2)			O8-H...O10	2.727(2)				
<b>Dy-1</b>	Dy1-O1	2.469(1)	Dy1-O3-C6	174.2(1)	<b>Ho-1</b>	Ho1-O1	2.458(1)	Ho1-O3-C6	174.5(1)
	Dy1-O2	2.506(1)	Dy1i-O4-C6	126.58(9)		Ho1-O2	2.494(1)	Ho1i-O4-C6	127.1(1)
	Dy1-O3	2.272(1)	Dy1-O5-C11	173.1(1)		Ho1-O3	2.261(1)	Ho1-O5-C11	173.0(1)
	Dy1-O4i	2.336(1)	Dy1ii-O6-C11	125.75(9)		Ho1-O4i	2.325(1)	Ho1ii-O6-C11	125.9(1)
	Dy1-O5	2.288(1)				Ho1-O5	2.281(1)		
	Dy1-O6ii	2.349(1)				Ho1-O6ii	2.340(1)		
	Dy1-O7	2.400(1)				Ho1-O7	2.385(1)		

	Dy1-O8	2.413(1)				Ho1-O8	2.400(1)		
	O7-H...O10	2.786(2)				O7-H...O10	2.780(3)		
	O8-H...O10	2.732(2)				O8-H...O10	2.731(2)		
<b>Er-1</b>	Er1-O1	2.447(1)	Er1-O3-C6	174.7(1)	<b>Tm-1</b>	Tm1-O1	2.434(2)	Tm1-O3-C6	175.2(2)
	Er1-O2	2.486(1)	Er1i-O4-C6	127.5(1)		Tm1-O2	2.476(2)	Tm1i-O4-C6	127.6(1)
	Er1-O3	2.248(1)	Er1-O5-C11	173.0(1)		Tm1-O3	2.238(2)	Tm1-O5-C11	173.1(2)
	Er1-O4i	2.317(1)	Er1ii-O6-C11	126.5(1)		Tm1-O4i	2.300(2)	Tm1ii-O6-C11	126.2(1)
	Er1-O5	2.268(1)				Tm1-O5	2.255(1)		
	Er1-O6ii	2.329(1)				Tm1-O6ii	2.316(2)		
	Er1-O7	2.377(1)				Tm1-O7	2.361(2)		
	Er1-O8	2.391(1)				Tm1-O8	2.377(2)		
	O7-H...O10	2.779(3)				O7-H...O10	2.779(4)		
O8-H...O10	2.732(3)			O8-H...O10	2.738(3)				
<b>Yb-1</b>	Yb1-O1	2.430(1)	Yb1-O3-C6	175.13(9)	<b>Lu-1</b>	Lu1-O1	2.416(4)	Lu1-O3-C6	176.0(4)
	Yb1-O2	2.473(1)	Yb1i-O4-C6	128.38(8)		Lu1-O2	2.456(4)	Lu1i-O4-C6	128.2(4)
	Yb1-O3	2.2296(9)	Yb1-O5-C11	173.24(8)		Lu1-O3	2.212(4)	Lu1-O5-C11	172.5(4)
	Yb1-O4i	2.282(1)	Yb1ii-O6-C11	126.97(8)		Lu1-O4i	2.282(4)	Lu1ii-O6-C11	127.4(4)
	Yb1-O5	2.2469(8)				Lu1-O5	2.221(3)		
	Yb1-O6ii	2.2986(9)				Lu1-O6ii	2.286(4)		
	Yb1-O7	2.355(1)				Lu1-O7	2.346(4)		
	Yb1-O8	2.371(1)				Lu1-O8	2.359(4)		
	O7-H...O10	2.776(2)				O7-H...O10	2.775(9)		
O8-H...O10	2.738(2)			O8-H...O10	2.735(8)				
<b>La-2</b>	La1-O1	2.567(2)	La1-O1-C1	142.7(2)					
	La1-O3	2.556(2)	La1-O3-C1	136.2(2)					
	La1-O4iii	2.499(2)	La1iii-O4-C6	147.6(2)					
	La1-O5	2.412(2)	La1-O5-C11	141.0(2)					
	La1-O6iv	2.428(2)	La1iv-O6-C11	142.3(2)					
	La1-O7	2.535(2)	La1-O7-C16	129.7(2)					
	La1-O8iv	2.461(2)	La1iv-O8-C16	145.5(2)					
	La1-O9	2.575(2)	La1-O9-C21	137.8(2)					
	O2-H...O3	2.608(3)							
O10-H...O7	2.621(3)								

Symmetry codes: (i)  $-x+1, -y+1, -z+1$ ; (ii)  $-x, -y+1, -z+1$ ; (iii)  $x, -y+1, z-\frac{1}{2}$ . (iv)  $x, -y+1, z+\frac{1}{2}$ .

### Powder X-Ray Diffraction Patterns of La-1 – Lu-1.

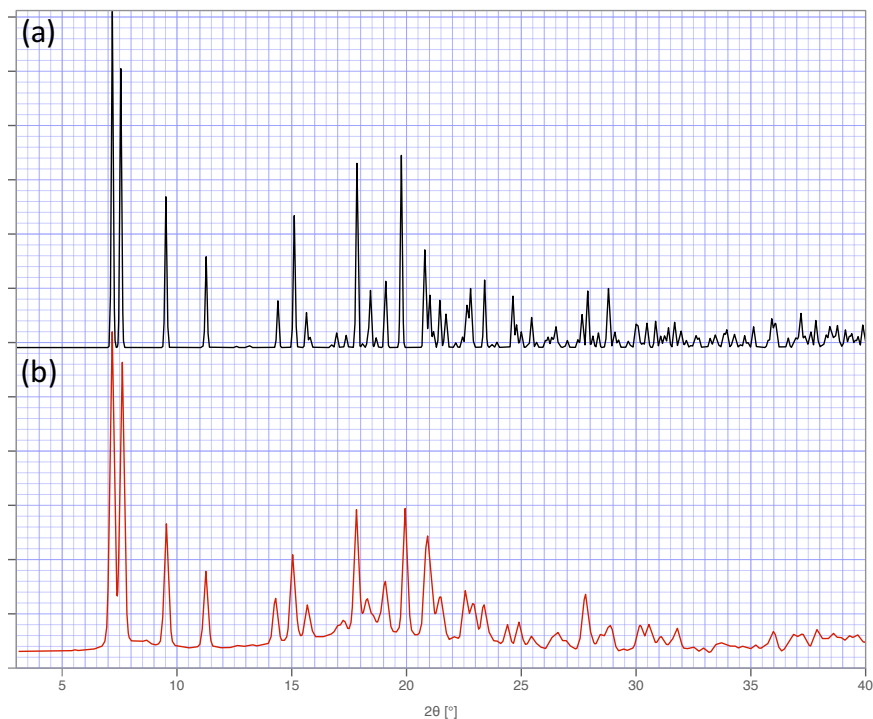


**Figure S16.** (a) Calculated and (b) experimental PXRD pattern of  $[(\text{La}(\text{TMC})_3(\text{H}_2\text{O})_2) \cdot (\text{HPy} \cdot \text{TMC})]_n$  (**La-1**). Experimental diffraction patterns were acquired using Cu  $K\alpha$  radiation.

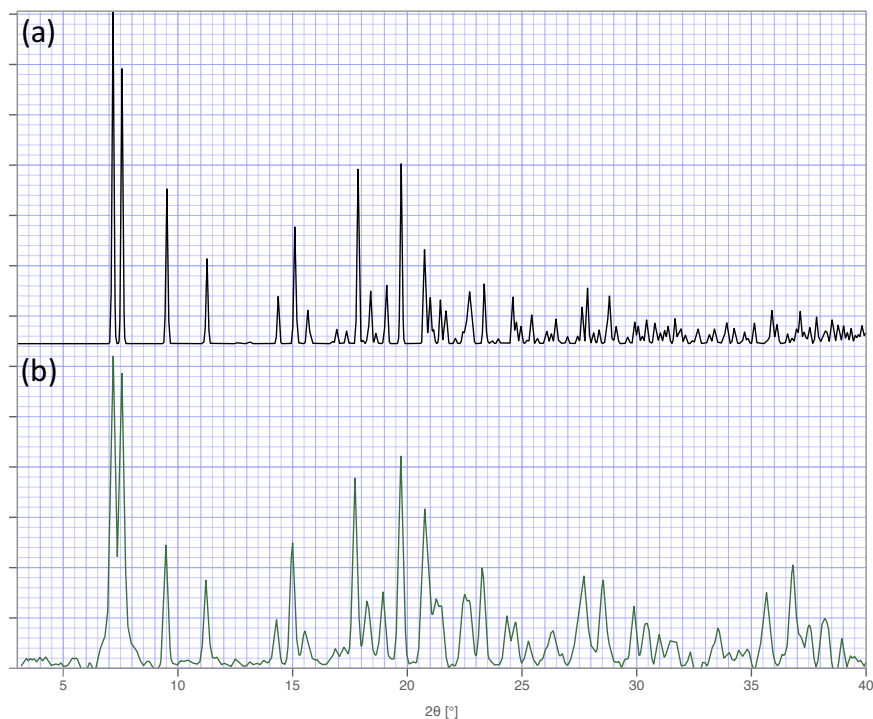


**Figure S17.** (a) Calculated and (b) experimental PXRD pattern of  $[(\text{Ce}(\text{TMC})_3(\text{H}_2\text{O})_2) \cdot (\text{HPy} \cdot \text{TMC})]_n$  (**Ce-1**). Experimental diffraction patterns were acquired using Cu  $K\alpha$  radiation.

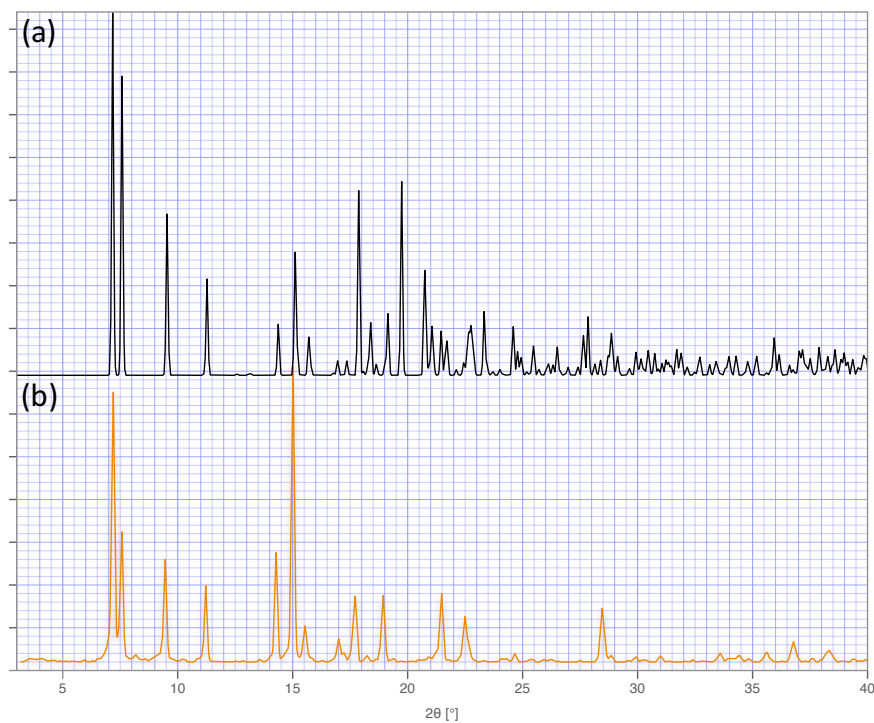


**Figure S18.** (a) Calculated and (b) experimental PXRD pattern of  $[(\text{Pr}(\text{TMC})_3(\text{H}_2\text{O})_2) \cdot (\text{HPy} \cdot \text{TMC})]_n$  (**Pr-1**). Experimental diffraction patterns were acquired using  $\text{Cu K}\alpha$  radiation.

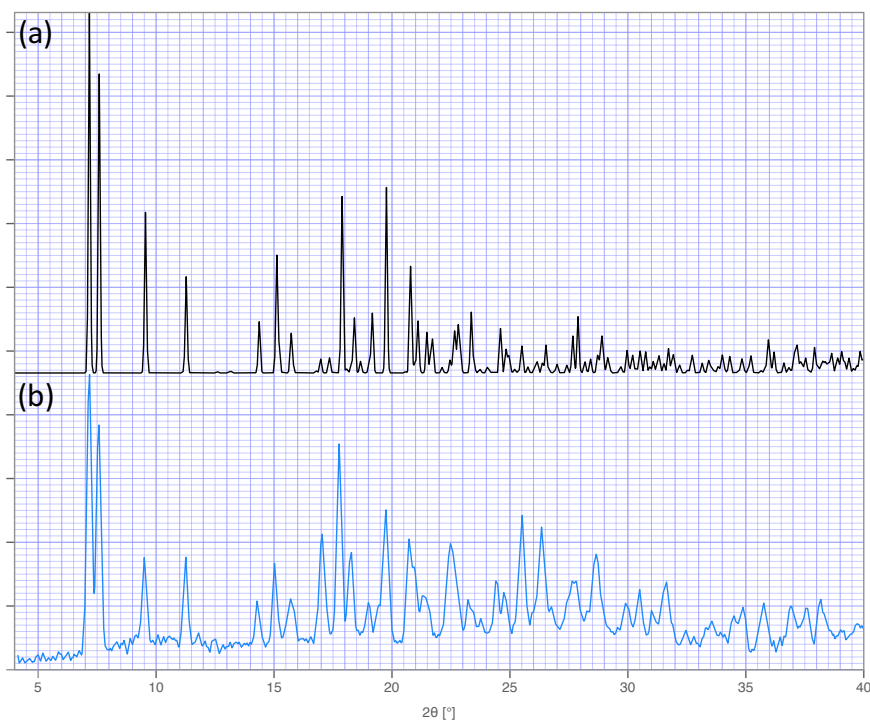


**Figure S19.** (a) Calculated and (b) experimental PXRD pattern of  $[(\text{Nd}(\text{TMC})_3(\text{H}_2\text{O})_2) \cdot (\text{HPy} \cdot \text{TMC})]_n$  (**Nd-1**). Experimental diffraction patterns were acquired using  $\text{Cu K}\alpha$  radiation.

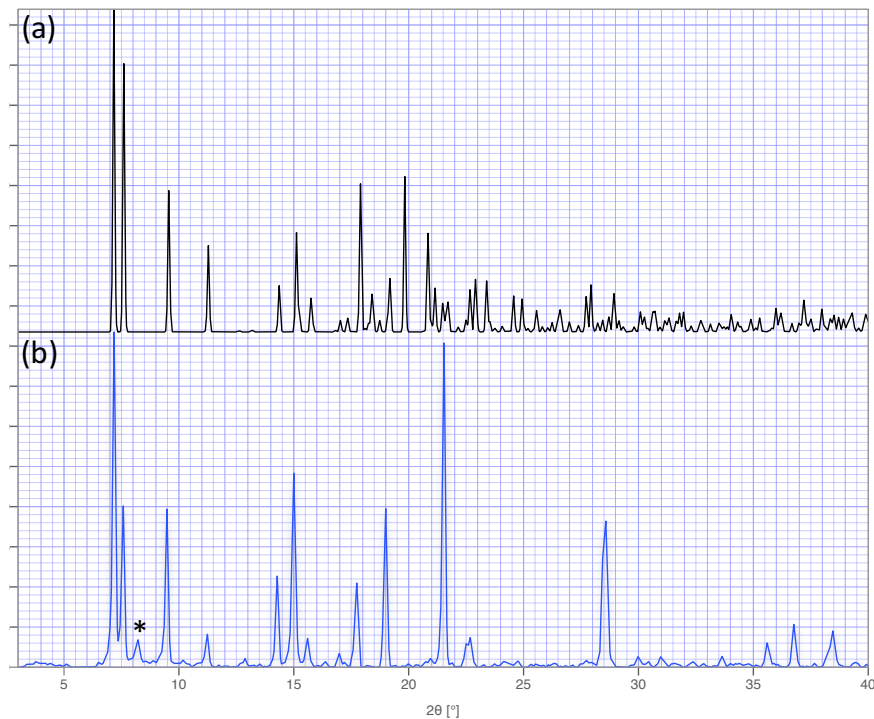


**Figure S20.** (a) Calculated and (b) experimental PXRD pattern of  $[(\text{Sm}(\text{TMC})_3(\text{H}_2\text{O})_2) \cdot (\text{HPy} \cdot \text{TMC})]_n$  (**Sm-1**). \*Peak appears due to disruption of lattice by drying and mechanical grinding. Experimental diffraction patterns were acquired using Cu  $K\alpha$  radiation.

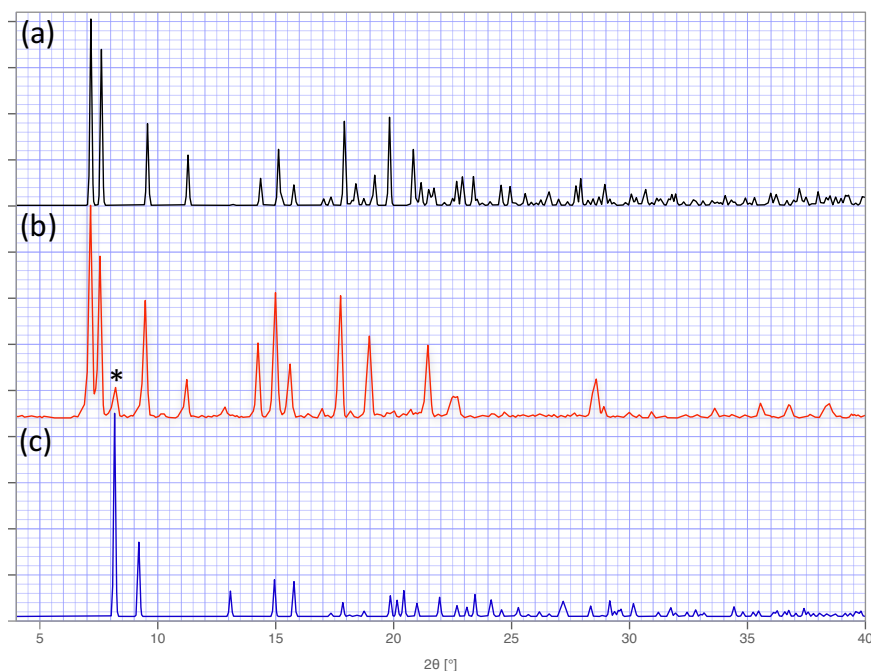


**Figure S21.** (a) Calculated and (b) experimental PXRD pattern of  $[(\text{Eu}(\text{TMC})_3(\text{H}_2\text{O})_2) \cdot (\text{HPy} \cdot \text{TMC})]_n$  (**Eu-1**). The pattern shown in (c) represents the calculated pattern for  $[\text{Eu}(\text{TMC})_3(\text{HTMC})_2]_n$ ; the dominant peaks in this diffraction pattern are in agreement with the impurity peaks seen in (b). \*Peak appears due to disruption of lattice by drying and mechanical grinding. Experimental diffraction patterns were acquired using Cu  $K\alpha$  radiation.

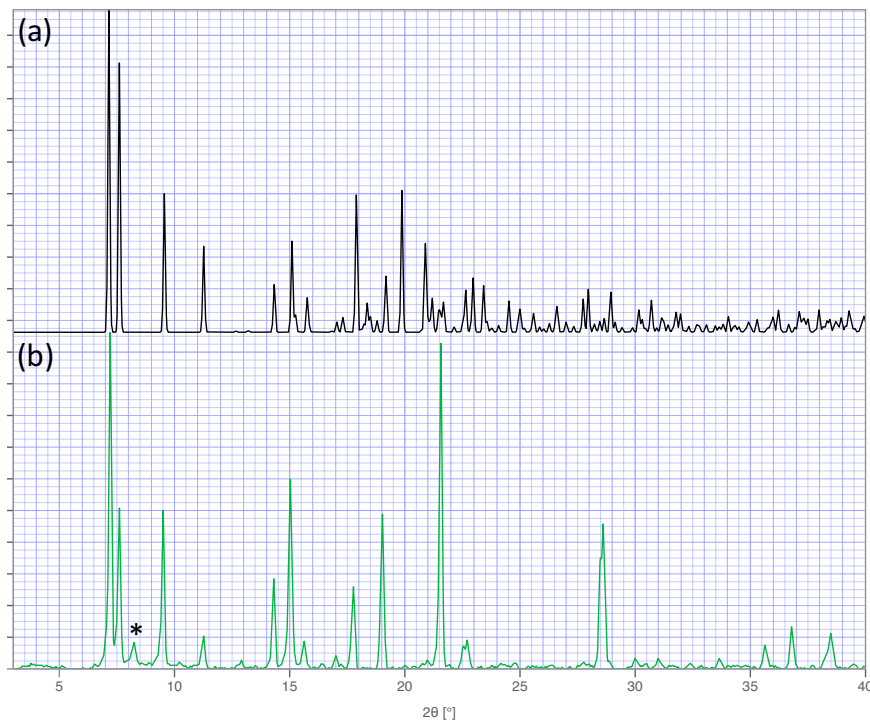


**Figure S22.** (a) Calculated and (b) experimental PXRD pattern of  $[(\text{Gd}(\text{TMC})_3(\text{H}_2\text{O})_2) \cdot (\text{HPy} \cdot \text{TMC})]_n$  (**Gd-1**). \*Peak appears due to disruption of lattice by drying and mechanical grinding. Experimental diffraction patterns were acquired using Cu  $K\alpha$  radiation.

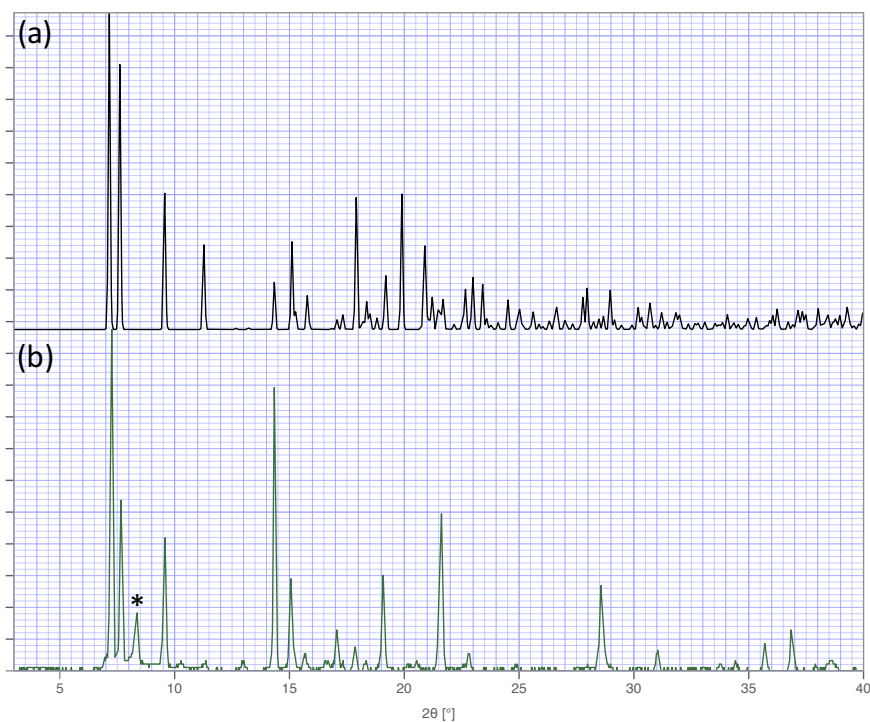


**Figure S23.** (a) Calculated and (b) experimental PXRD pattern of  $[(\text{Tb}(\text{TMC})_3(\text{H}_2\text{O})_2) \cdot (\text{HPy} \cdot \text{TMC})]_n$  (**Tb-1**). \*Peak appears due to disruption of lattice by drying and mechanical grinding. Experimental diffraction patterns were acquired using Cu  $K\alpha$  radiation.

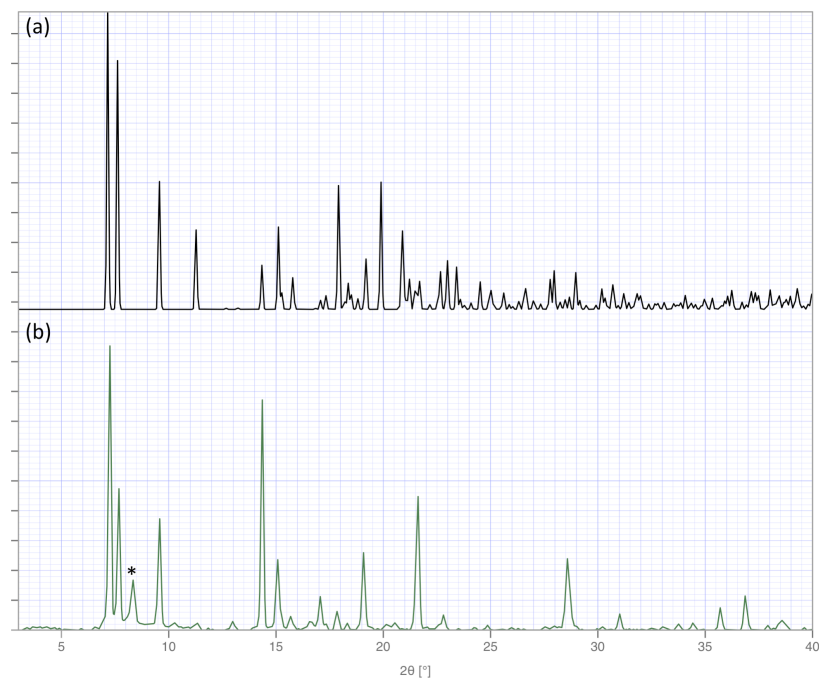


**Figure S24.** (a) Calculated and (b) experimental PXRD pattern of  $[(\text{Dy}(\text{TMC})_3(\text{H}_2\text{O})_2) \cdot (\text{HPy} \cdot \text{TMC})]_n$  (**Dy-1**). \*Peak appears due to disruption of lattice by drying and mechanical grinding. Experimental diffraction patterns were acquired using Cu  $K\alpha$  radiation.

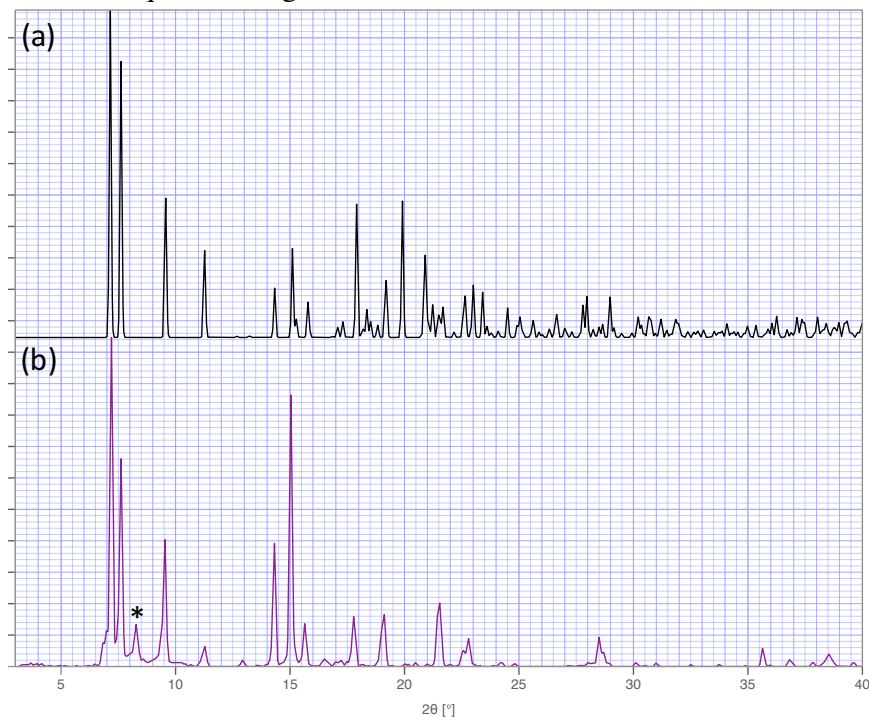


**Figure S25.** (a) Calculated and (b) experimental PXRD pattern of  $[(\text{Ho}(\text{TMC})_3(\text{H}_2\text{O})_2) \cdot (\text{HPy} \cdot \text{TMC})]_n$  (**Ho-1**). \*Peak appears due to disruption of lattice by drying and mechanical grinding. Experimental diffraction patterns were acquired using Cu  $K\alpha$  radiation.

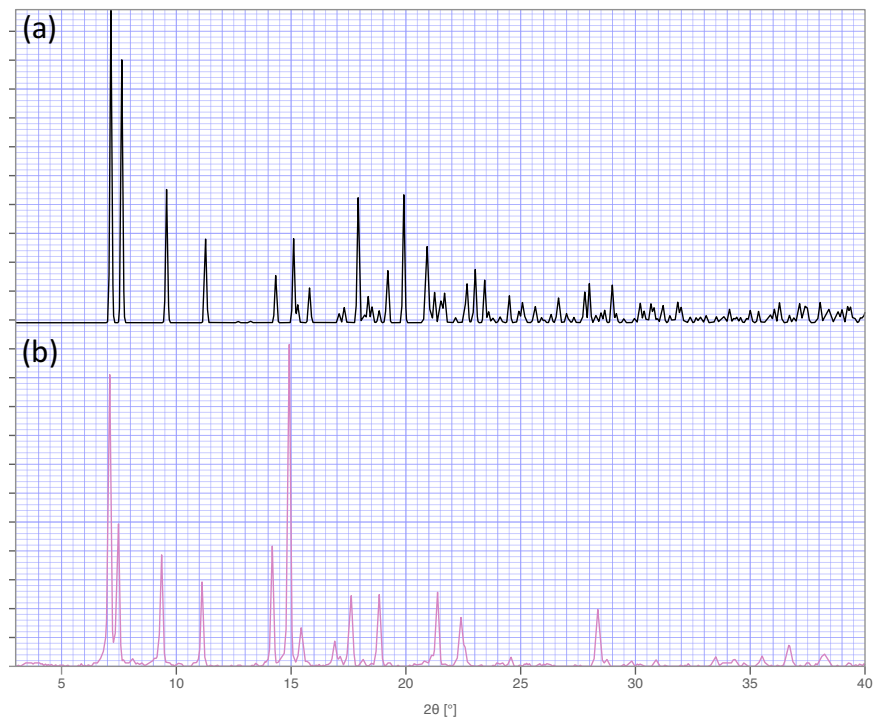


**Figure S26.** (a) Calculated and (b) experimental PXRD pattern of  $[(\text{Er}(\text{TMC})_3(\text{H}_2\text{O})_2) \cdot (\text{HPy} \cdot \text{TMC})]_n$  (**Er-1**). Experimental diffraction patterns were acquired using  $\text{Cu K}\alpha$  radiation.

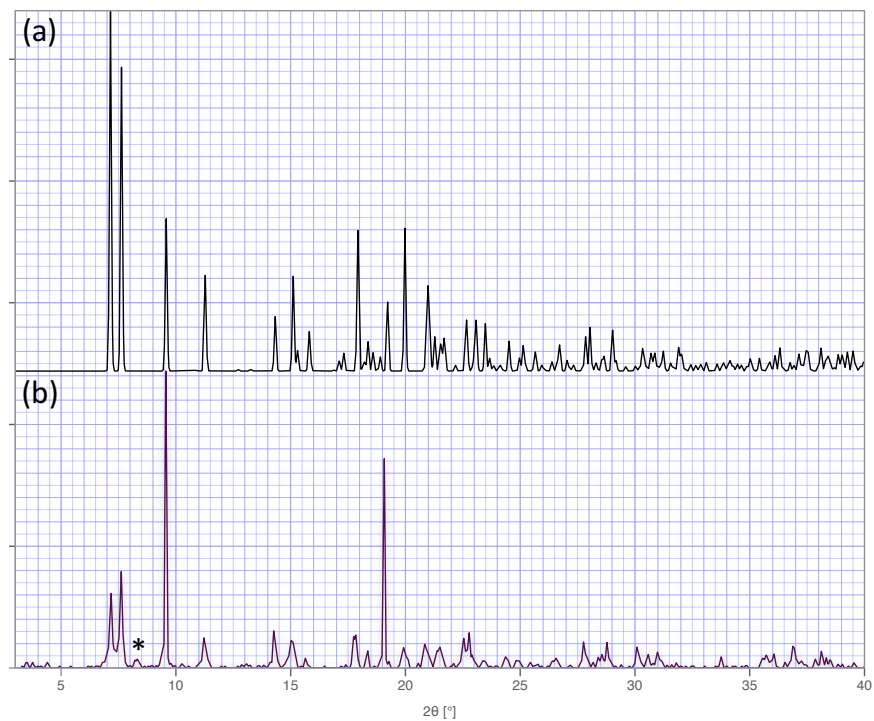


**Figure S27.** (a) Calculated and (b) experimental PXRD pattern of  $[(\text{Tm}(\text{TMC})_3(\text{H}_2\text{O})_2) \cdot (\text{HPy} \cdot \text{TMC})]_n$  (**Tm-1**). \*Peak appears due to disruption of lattice by mechanical grinding. Experimental diffraction patterns were acquired using  $\text{Cu K}\alpha$  radiation.

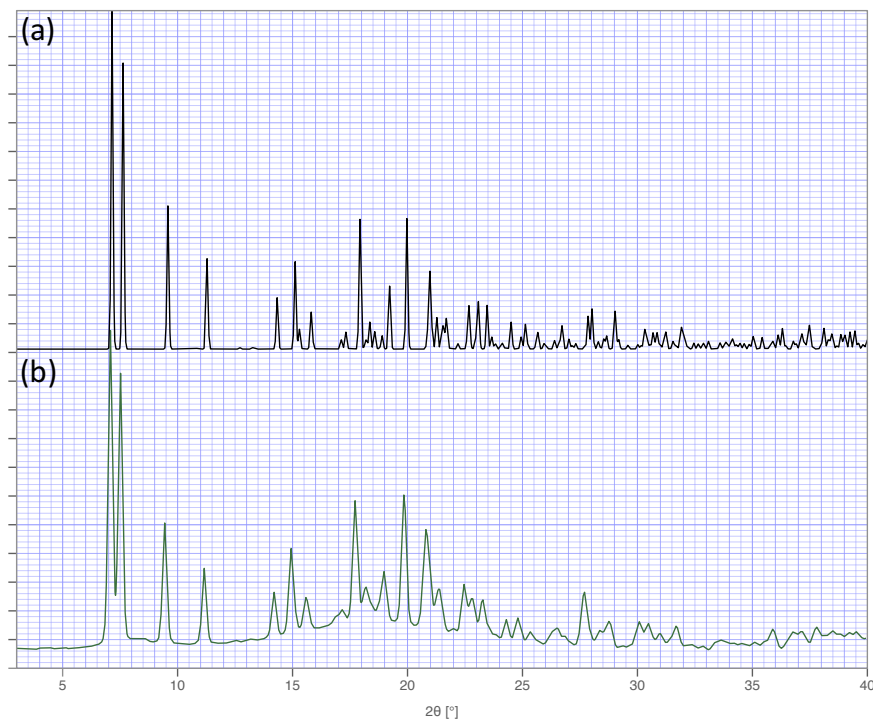


**Figure S28.** (a) Calculated and (b) experimental PXRD pattern of  $[(\text{Yb}(\text{TMC})_3(\text{H}_2\text{O})_2) \cdot (\text{HPy} \cdot \text{TMC})]_n$  (**Yb-1**). Experimental diffraction patterns were acquired using Cu  $K\alpha$  radiation.

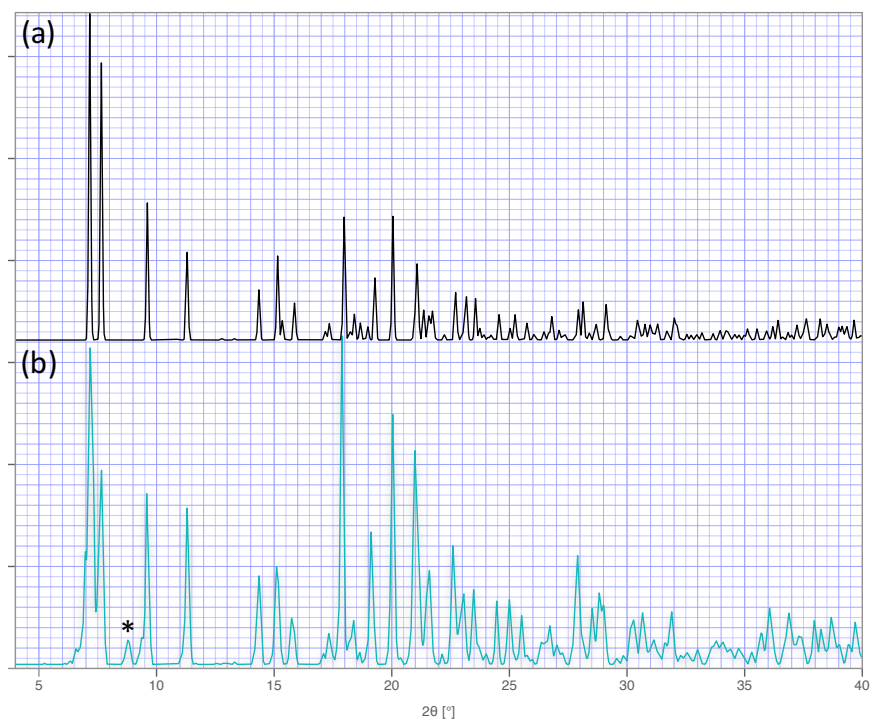


**Figure S29.** (a) Calculated and (b) experimental PXRD pattern of  $[(\text{Lu}(\text{TMC})_3(\text{H}_2\text{O})_2) \cdot (\text{HPy} \cdot \text{TMC})]_n$  (**Lu-1**). \*Peak appears due to disruption of lattice by drying and mechanical grinding. Experimental diffraction patterns were acquired using Cu  $K\alpha$  radiation.

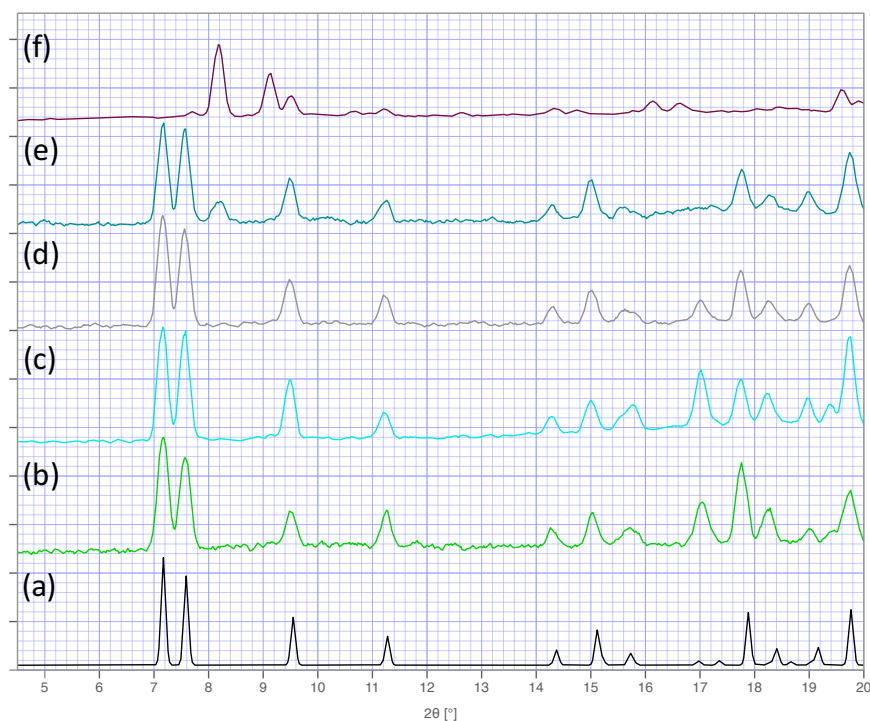


**Figure S30.** Calculated PXRD pattern from  $[(\text{Nd}(\text{TMC})_3(\text{H}_2\text{O})_2) \cdot (\text{HPy} \cdot \text{TMC})]_n$  (**Nd-1**) single crystal data; (b) PXRD pattern acquired on single crystal material; (c) PXRD of single crystals dried under vacuum; (d) PXRD of single crystals after mechanical grinding; (e) PXRD of single crystals after drying under vacuum and mechanical grinding; (f) PXRD of single crystals after triturating five times with ethanol. The common impurity peak at  $8.3^\circ$  appears only after drying and mechanical grinding (e), and becomes the dominant signal upon repeated washes with ethanol (f). Experimental diffraction patterns were acquired using Cu  $K\alpha$  radiation.

### Emission and Excitation Spectra of La-1 – Lu-1.

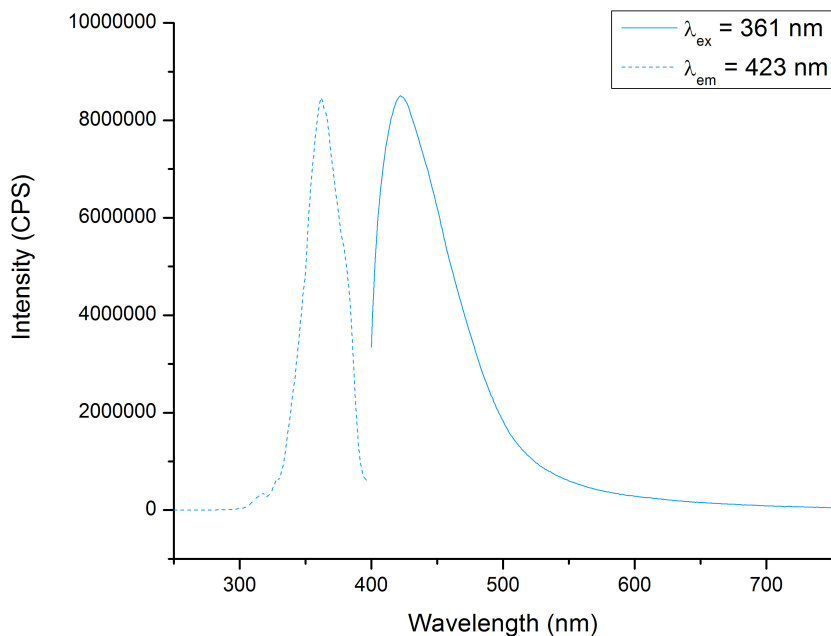


**Figure S31.** Excitation (---) and visible emission (—) spectrum of 2-thiophenecarboxylic acid (HTMC).

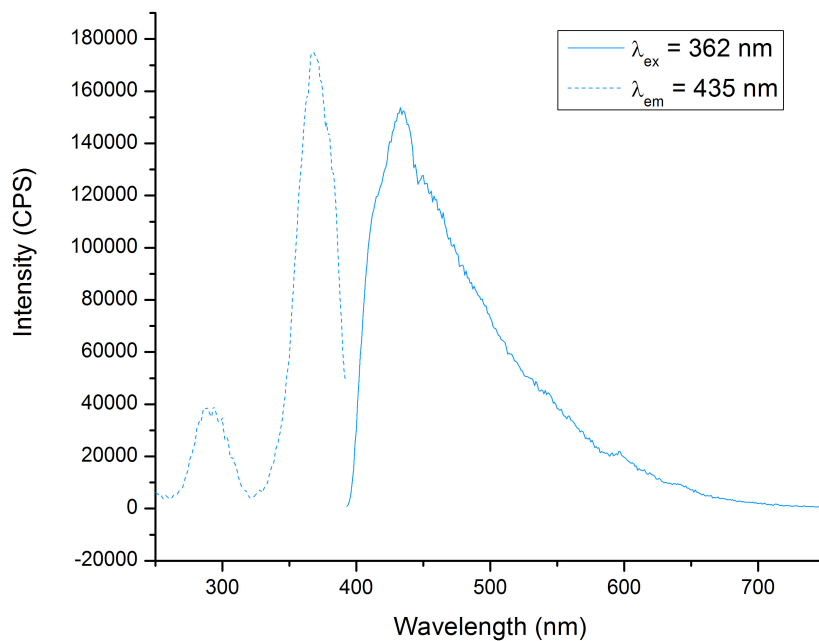


**Figure S32.** Excitation (---) and visible emission (—) spectrum of  $[(Ce(TMC)_3(H_2O)_2) \cdot (HPy \cdot TMC)]_n$  (Ce-1).

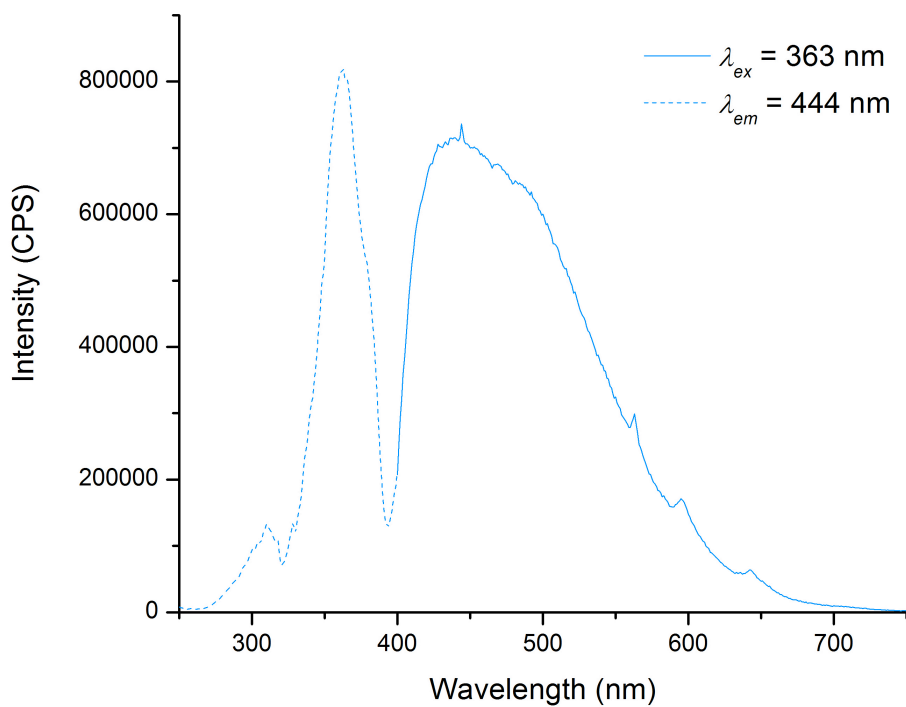


**Figure S33.** Excitation (---) and visible emission (—) spectrum of  $[(\text{Sm}(\text{TMC})_3(\text{H}_2\text{O})_2) \cdot (\text{HPy} \cdot \text{TMC})]_n$  (**Sm-1**).

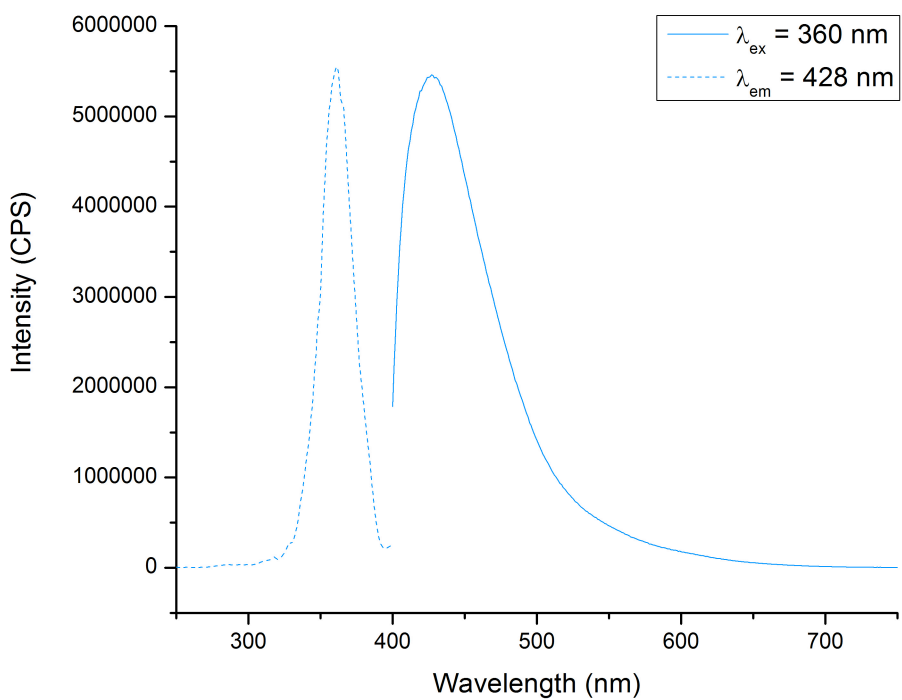


**Figure S34.** Excitation (---) and visible emission (—) spectrum of  $[(\text{Gd}(\text{TMC})_3(\text{H}_2\text{O})_2) \cdot (\text{HPy} \cdot \text{TMC})]_n$  (**Gd-1**).

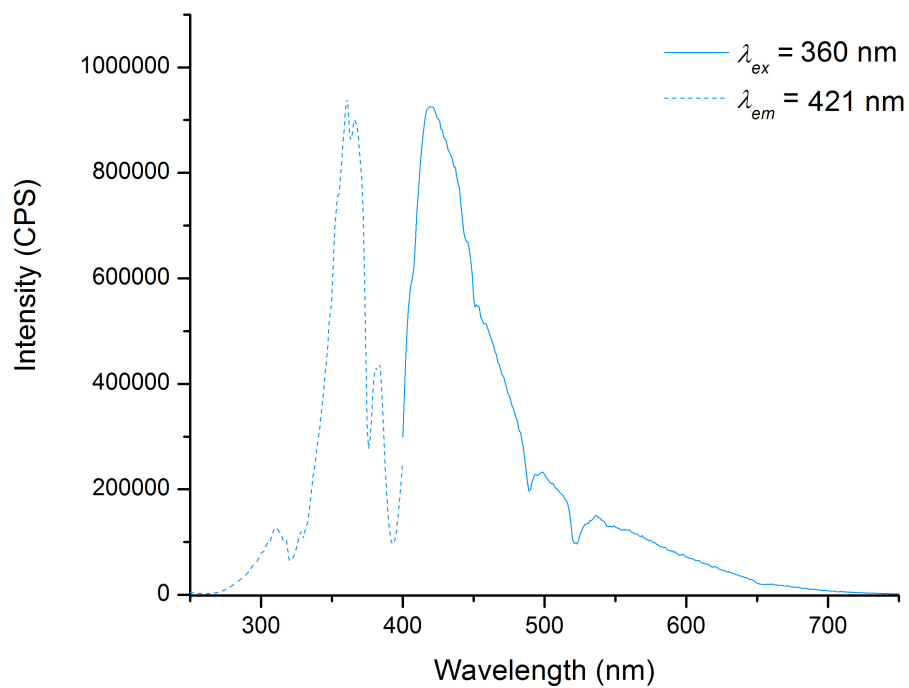


**Figure S35.** Excitation (---) and visible emission (—) spectrum of  $[(\text{Er}(\text{TMC})_3(\text{H}_2\text{O})_2) \cdot (\text{HPy} \cdot \text{TMC})]_n$  (**Er-1**).

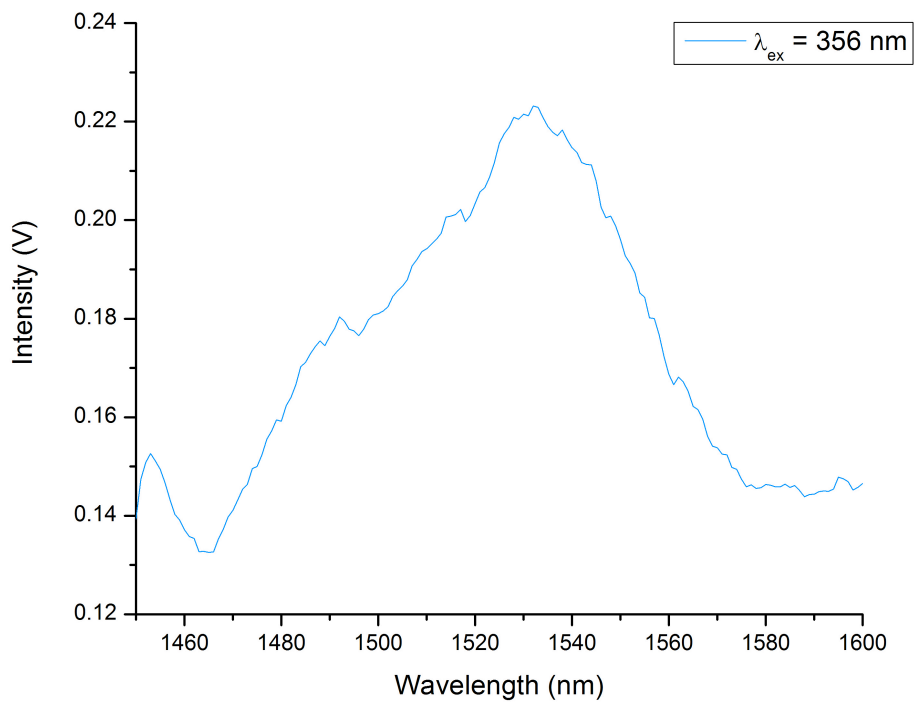


**Figure S36.** NIR emission spectrum of  $[(\text{Er}(\text{TMC})_3(\text{H}_2\text{O})_2) \cdot (\text{HPy} \cdot \text{TMC})]_n$  (**Er-1**).

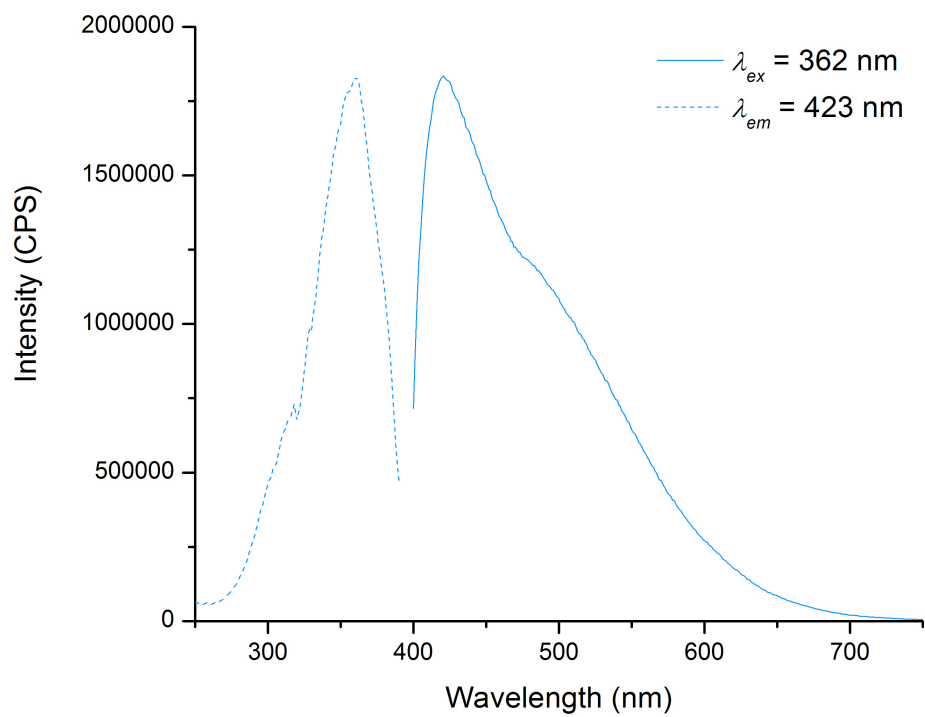


**Figure S37.** Excitation (---) and visible emission (—) spectrum of  $[(\text{Tm}(\text{TMC})_3(\text{H}_2\text{O})_2) \cdot (\text{HPy} \cdot \text{TMC})]_n$  (**Tm-1**).

### Raman Fluorescence.

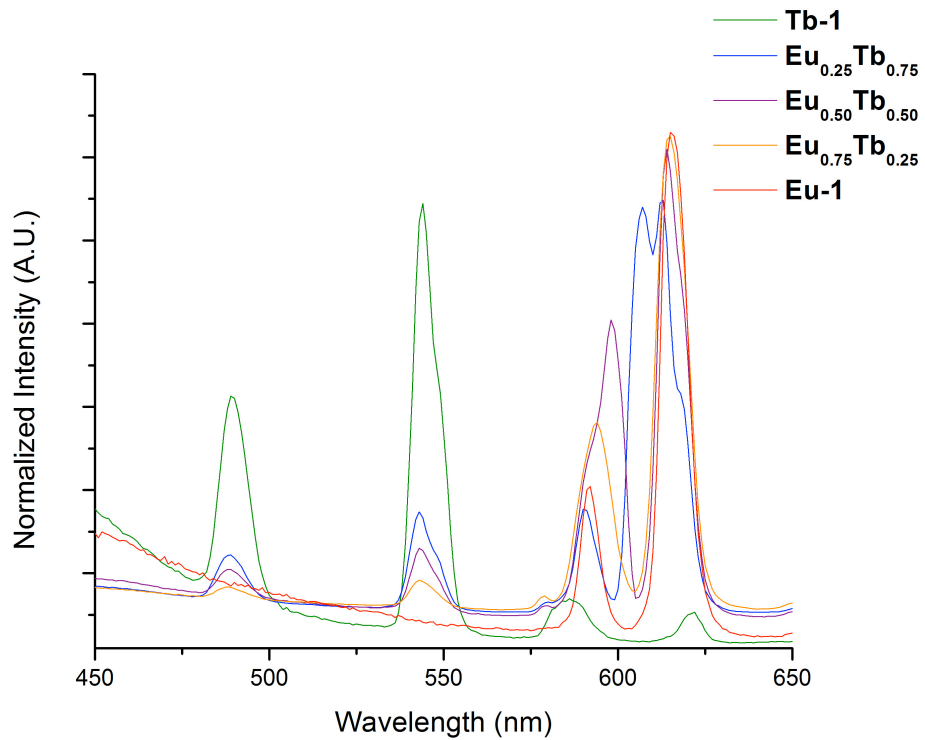


**Figure S38.** Emission spectra collected for single crystals of the mixed europium:terbium phases using the Raman laser. The excitation wavelength used for each acquisition was 355 nm.

### Time-Resolved Fluorescence Lifetime Measurements.

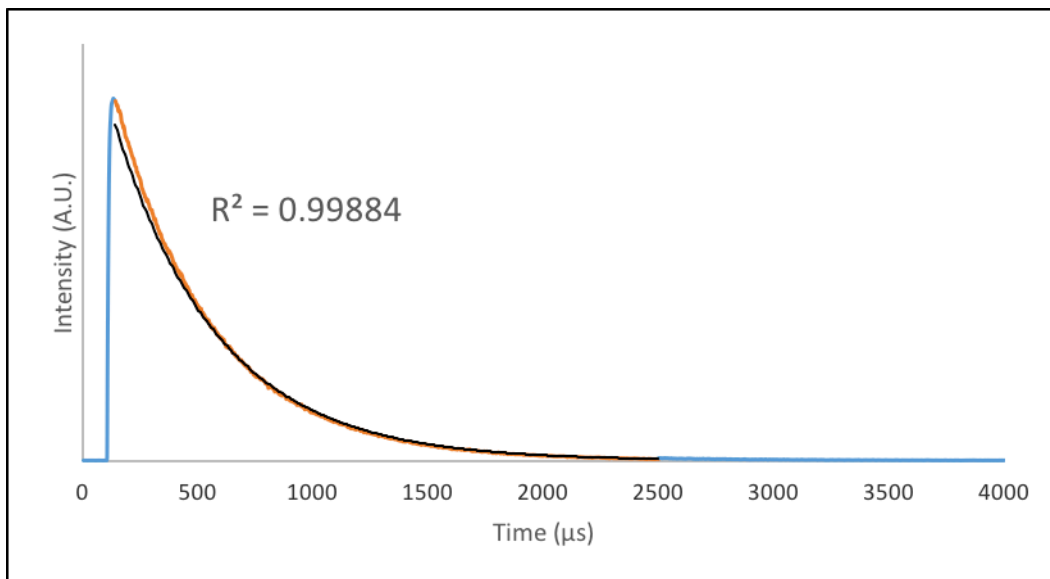


**Figure S39.** Lifetime decay curve of  $[(\text{Eu}(\text{TMC})_3(\text{H}_2\text{O})_2) \cdot (\text{HPy} \cdot \text{TMC})]_n$  (**Eu-1**) irradiated with 360 nm light. The area of the curve used to calculate the decay rate is marked as the red line. The black line denotes the fit of the exponential curve.

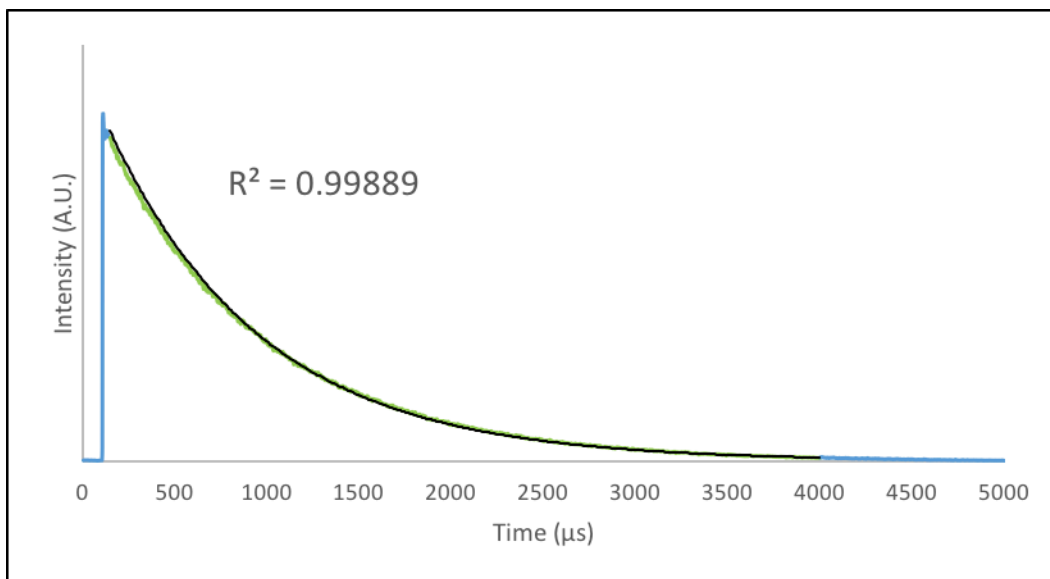


**Figure S40.** Lifetime decay curve of  $[(\text{Tb}(\text{TMC})_3(\text{H}_2\text{O})_2) \cdot (\text{HPy} \cdot \text{TMC})]_n$  (**Tb-1**) irradiated with 367 nm light. The area of the curve used to calculate the decay rate is marked as the green line. The black line denotes the fit of the exponential curve.

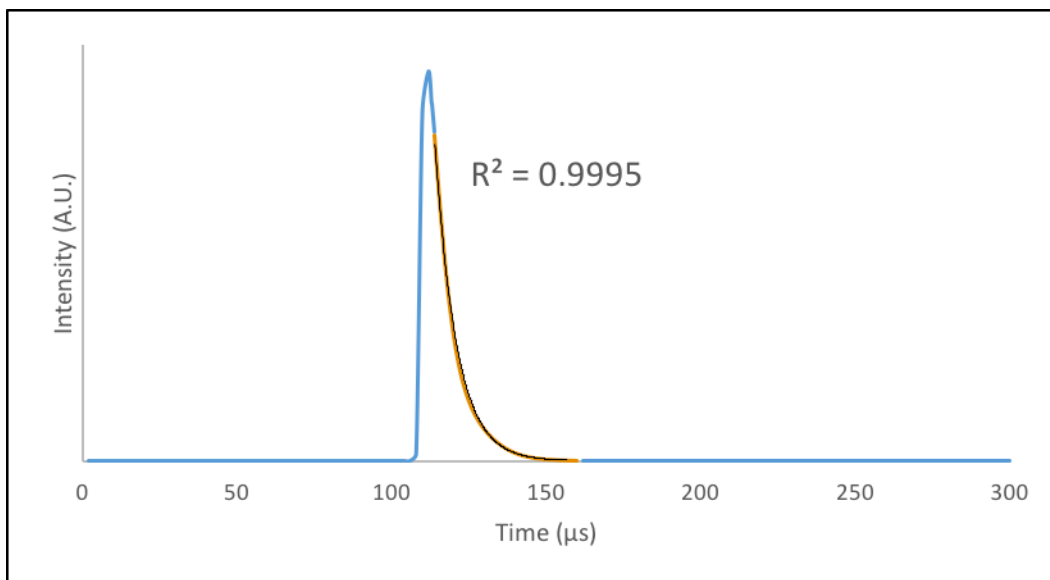


**Figure S41.** Lifetime decay curve of  $[(\text{Dy}(\text{TMC})_3(\text{H}_2\text{O})_2) \cdot (\text{HPy} \cdot \text{TMC})]_n$  (**Dy-1**) irradiated with 362 nm light. The area of the curve used to calculate the decay rate is marked as the orange line. The black line denotes the fit of the exponential curve.

## Thermal Stability Measurements

The sample was prepared first by drying under dynamic vacuum at 70 °C, then analyzed by thermogravimetric analysis under a flow of dinitrogen gas at a rate of 10 mL min<sup>-1</sup>, and the temperature ramped up to 500 °C at a rate of 5 °C min<sup>-1</sup>; the resulting TGA curve for the thermal decomposition of [(Pr(TMC)<sub>3</sub>)·(HPy·TMC)]<sub>n</sub> is presented below.

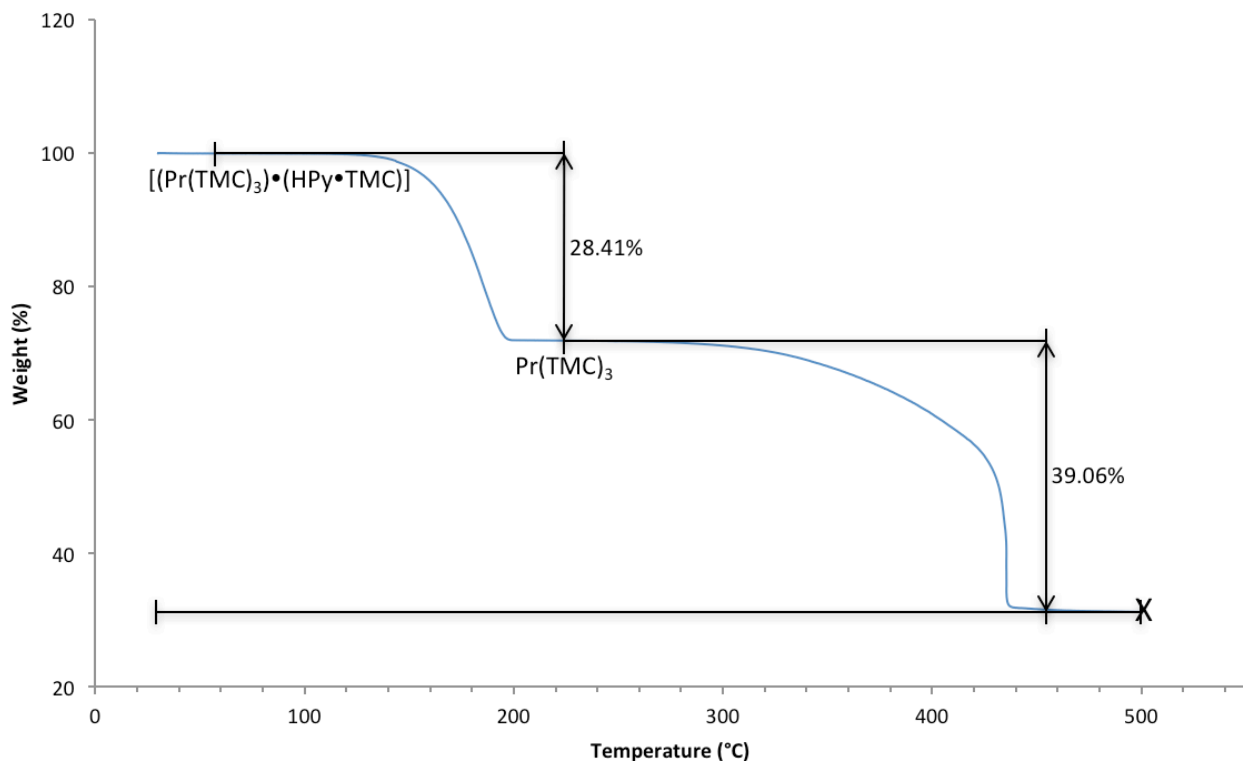


**Figure S42.** TGA curve obtained for [(Pr(TMC)<sub>3</sub>)·(HPy·TMC)]<sub>n</sub> under dinitrogen flow. Two mass losses are present in the range of 130-195 and 250-435 °C, corresponding to a 28.41 and 39.06% mass loss, respectively.

1. Yuan, L.; Yin, M.; Yuan, E.; Sun, J.; Zhang, K., *Inorganica Chimica Acta* **2004**, *357*, 89-94.